UNIVERSITY OF TWENTE.

UMC Utrecht

Master's Thesis Technical Medicine

3D printed guided positioning of extreme pedicle screws to aid in vertebral derotation

A feasibility cadaver study to improve scoliosis surgery

Diederik P.D. Suurd

13 October 2017

Faculty of Science and Technology

Internship at:
Department of Orthopaedic Surgery
University Medical Center Utrecht

Thesis committee
Chairman – dr. ir. F. van der Heijden, University of Twente
Medical supervisor – dr. M.C. Kruyt, MD, UMC Utrecht
Technical supervisor – ir. E.E.G. Hekman, University of Twente
Mentor – drs. A.G. Lovink, University of Twente
Additional member – A. Swaan, MSc, University of Amsterdam
External member – dr. ir. F. van der Heijden, University of Twente

---

ABSTRACT

Objective: In scoliosis correction derotation of the vertebrae is challenging, resulting in non-ideal rotational alignment of the vertebrae, which is associated with postoperative rib prominence and patients cosmetic dissatisfaction. Nowadays, unconventional pedicle screw trajectories can be planned with the advent of 3D printed guiding techniques. We studied the potential of preplanned extreme screw positions to aid in vertebral rotation and the use of 3D printed patient-specific drill guides. Hypothetically, the amount of rotation of a vertebra increases by an increased offset between pedicle screw head and the rod.

Methods: The study is a feasibility study in a human cadaver (age 57). Volumes of the vertebrae are reconstructed from a boneMRI protocol. The volumes are used for 3D trajectory planning and manufacturing a patient-specific 3D printed drill guide, named SpineGuide. Six sections of three vertebrae represented the test situation where cephalad en caudal vertebrae were fixed. The middle vertebra was instrumented with an extreme screw on one side. Screw positioning was realized with the aid of the SpineGuide. Pre-bent CoCr rods were used to gain more vertebral rotation. Thereby, forces acting on the screw-rod construct were measured with a torque wrench during instrumentation and calculated using a FEM simulation. After instrumentation, a CT scan was used to analyze drill guide accuracy and the translational and rotational movement of the middle vertebra.

Results: *Pedicle screw placement:* In total 24 screws were inserted with the SpineGuide; 5 extreme pedicle screw trajectories and 19 conventional pedicle screw trajectories. 11 of the 19 conventional screws were correctly placed using the SpineGuide. 8 screws had incorrect placement (5 Grade 1; 2 Grade 2; 1 Grade 3). *Derotation maneuver:* 4 out of 5 of the extreme pedicle screws were pulled out during the rotational maneuver. One extreme pedicle screw was not pulled out. However, derotation of the instrumented vertebra was not observed.

Discussion: Extreme pedicle screw placement is feasible. However, extreme screw trajectories are not optimal which led to high pull-out ratio. This may be related to the bone quality and high force nonaxial loading of the pedicle screw. Planning of extreme pedicle screws the SpineGuide needs to be improved for higher success percentage. Derotation of the only vertebra with a correct placed extreme pedicle screw was not observed. Further research is needed with improved extreme pedicle screw placement to aid in vertebral derotation.

SAMENVATTING

Doel: Tijdens een scoliose correctie is het deroteren van de wervels vaak uitdagend en kan dit resulteren in een niet ideale uitlijning van hoe de wervels georiënteerd zijn. Dit is geassocieerd met postoperatieve ribprominentie en cosmetische ontevredenheid van de patiënt. Met de huidige technieken van 3D printen is het mogelijk om niet conventionele pedikelschroef trajecten te plannen en te realiseren met de hulp van boormallen. We hebben het potentieel van vooraf geplande extreme schroef posities onderzocht, die mogelijk ondersteunen bij wervel rotatie. Daarbij hebben we het gebruik van 3D geprinte boormallen onderzocht. Wij hypothetiseren dat de hoeveelheid rotatie van een wervel groter door een grote afstand tussen pedikelschroefkop en de staaf.

Methode: De studie is een haalbaarheidsstudie op een menselijke kadaver (leeftijd 57). Volumes van de wervels zijn reconstrueert uit MRI data. De volumes van de wervels zijn gebruikt voor het 3D plannen van schroeftrajecten en voor het maken van een patiënt specifieke 3D geprinte boormal, genoemd SpineGuide. Secties van drie wervels representeerde de test situatie, waarbij de cephale en caudale wervel gefixeerd was. De middelste wervel werd geïnstrumenteerd met een extreme schroef aan één kant. Het positioneren van de schroef werd gedaan met behulp van de SpineGuide. Een vooraf gebogen CoCr staaf werd gebruikt voor het behalen van meer wervel rotatie. Daarbij werden ook de krachten die op het schroef-staaf systeem werkten gemeten met een momentsleutel gedurende de instrumentatie en werden deze krachten berekend met behulp van een FEM simulatie. Na de instrumentatie werd er een CT scan gemaakt om the accuraatheid van de SpineGuide te bepalen en om de translatie en rotatie van de middelste wervel te meten.

Resultaten: *Pedikelschroef plaatsing:* In totaal zijn er 24 schroeven ingebracht met een SpineGuide; 5 extreme trajecten en 19 conventionele pedikelschroef trajecten. 11 van de 19 conventionele schroeven waren correct geplaatst met de SpineGuide. 8 schroeven hadden een incorrecte plaatsing (5 Graad 1; 2 Graad 2; 1 Graad 3). *Derotatie maneuver:* 4 van de 5 extreme pedikelschroeven werden eruit getrokken gedurende de rotatie maneuver. Eén extreme pedikelschroef was er niet uitgetrokken, maar derotatie van de geïnstrumenteerde wervel was niet gezien.

Discussie: Extreme pedikelschroef plaatsing is haalbaar, maar extreme schroef trajecten zijn niet optimaal, waardoor er een hoog uitbreek ratio was. Dit is mogelijk gerelateerd aan de botkwaliteit van het kadaver en door niet axiale ladingskracht op de schroef. Het plannen van extreme pedikelschroeven met gebruik van de SpineGuide moet verder verbeterd worden voor een hoger succes percentage van plaatsing. Derotatie van de enige wervel met een correct geplaatste extreme schroef was niet gezien. Verder onderzoek is nodig voor het verbeteren van de extreme pedikelschroef plaatsing voor derotatie van de wervel.

TABLE OF CONTENTS

Abstract 0
Samenvatting 2
Table of Contents 3
1 Introduction 5
1.1 Clinical relevance 5
1.2 Previous UMC Utrecht research 5
1.3 Medical background 6
1.3.1 Anatomy of the spinal column 6
1.3.2 Scoliosis and surgery 7
1.3.3 Vertebral derotation 9
1.4 Technical background 10
1.4.1 Biomechanics of axial derotation 10
1.5 Thesis outline 11
2 Materials and Methods 13
2.1 Study overview 13
2.2 Material collection & preparation 13
2.2.1 Specimen 13
2.2.2 Medical image acquisition 13
2.2.3 Manufacturing SpineGuide 13
2.2.4 Spinal instrumentation 15
2.2.5 Calibration cricket 15
2.3 Cadaveric feasibility study 16
2.3.1 Screw placement 16
2.3.2 Experimental setup for derotation 16
2.3.3 Axial derotation maneuver with extreme screw positioning 17
2.3.4 CT acquisitions 18
2.4 Analysis 19
2.4.1 SpineGuide accuracy 19
2.4.2 Axial derotation maneuver with extreme positioned pedicle screw 19
3 Results 20
3.1 SpineGuide accuracy 20
3.2 Axial derotation with extreme positioned pedicle screw 22
4 Discussion 24
4.1 Summary 24

4.2 SpineGuide accuracy 24
4.3 Axial derotation with extreme screw positioning 25
4.4 Conclusion 27
4.5 Future work 27
5 Acknowledgements 29
6 References 30
7 Appendix 34
7.1 Appendix 1 – Segmentation vertebrae MeVisLab 34
7.2 Appendix 2 – Trajectory planning SolidWorks 34
7.3 Appendix 3 – SpineGuide design SolidWorks 35
7.4 Appendix 4 – Calibration cricket 36
7.5 Appendix 5 – FEM simulation by Kuiper 37
7.5.1 Research Objective 37
7.5.2 Finite Element Method 37
7.6 Appendix 6 – SpineGuide accuracy analysis 38
7.7 Appendix 7 – Torque measurements 39

1 INTRODUCTION

1.1 CLINICAL RELEVANCE

Scoliosis is a 3D deformity of the spine. Posterior correction surgery with two rods is the most common surgical intervention for scoliosis and is a precise and challenging task. Changes in the shape of the spine and dysplastic vertebrae make correction surgery and the insertion of pedicle screws difficult. One aim of the surgery is to prevent worsening of the deformities, and a sub-aim is improving the cosmesis [1]. Besides, it is hard to predict how the surgery results in the sagittal, coronal and axial correction of the spine. Especially derotation of the (apical) vertebra during surgery is often difficult, resulting in non-ideal rotational alignment of the vertebrae. The rotated vertebrae in scoliosis and the connected ribs produce anterior rib cage prominence, posterior rib hump (gibbus) and scapular prominence [2]. Non-ideal rotational alignment could thus result in postoperative rib prominence and patients cosmetic dissatisfaction [2,3].

With the advent of 3D printing techniques it is possible to create patient-specific drill guides matching the anatomy [4–23]. These guides can be used to plan and safely insert pedicle screws during scoliosis surgery with a high accuracy. A big advantage of the drill guides is the preoperative planning and, thereby, the use of drill guides make it possible to insert and reproduce unconventional, more extremely placed, pedicle screw trajectories, figure 1. These preplanned extreme trajectories, for instance, can be used for vertebral derotation and may aid in current derotation techniques to decrease postoperative rib prominence and patients cosmetic dissatisfaction. We studied the potential of preplanned extreme pedicle screw trajectories using patient-specific drill guides to aid in vertebral rotation.

Figure 1 – a) A conventional pedicle screw trajectory and b) an extreme pedicle screw trajectory.

1.2 PREVIOUS UMC UTRECHT RESEARCH

The orthopedic department in the UMC Utrecht focuses part of its research on making (scoliosis) spine surgery safer and better. One of the goals is to reduce the radiation dose given to patients with scoliosis. Another focus is the increased use of personalized medicine, like patient-specific 3D guiding techniques in today's operating rooms. A great example is the Smith & Nephew Visionaire MRI based patient-specific cutting guide for total knee arthroplasty [24]. This put dr. Kruyt, an orthopedic surgeon in the UMC Utrecht, on the mind to use an MRI based patient-specific drill guides to safely insert pedicle screws during (scoliosis) surgery. Therefore, in 2012 Technical Medicine intern Swaan (University of Twente (UT)) developed an MRI based patient-specific drill guide for implanting pedicle screws in the thoracic spine, referred to as the SpineGuide (figure 2a) [25]. The MRI techniques developed rapidly between Swaan's work and nowadays, resulting in cooperation with UMC Utrecht spinoff MRIguidance, who make it able to visualize cortical bone with MRI [26]. They offer an MRI technique in which bone and soft tissue simultaneously are visualized during one MRI exam, without the harm of radiation. One of their goals is to offer orthopedic surgeons improved tools for diagnosis and personalized treatment planning. The ability to create 3D volumes out of the boneMRI is valuable for 3D treatment planning like patient-specific drill guides. Especially in children and adolescents, this is an advantage; because their radiation exposure should be minimized to decrease the risk of cancer. Technical Medicine intern Geldof (UT) researched the segmentation accuracy of boneMRI compared with CT for the manufacturing of MRI based SpineGuides [27]. Thereby, cooperation with Holland Innovative, a company specialized in (medical) product development, and TechMed Proeftuin (UT) gave rise to the further development of the SpineGuide [28]. Industrial Design intern Drost (Saxion University of Applied Sciences) further developed the SpineGuide to not only project the accurate drill trajectory, but also be user-friendly for the surgeon, figure 2b [29]. He interviewed orthopedic surgeons to improve the design based on the surgeon's use of drill guides and to gain knowledge about more stability via support blocks. The insights gained in these projects are used in this thesis.

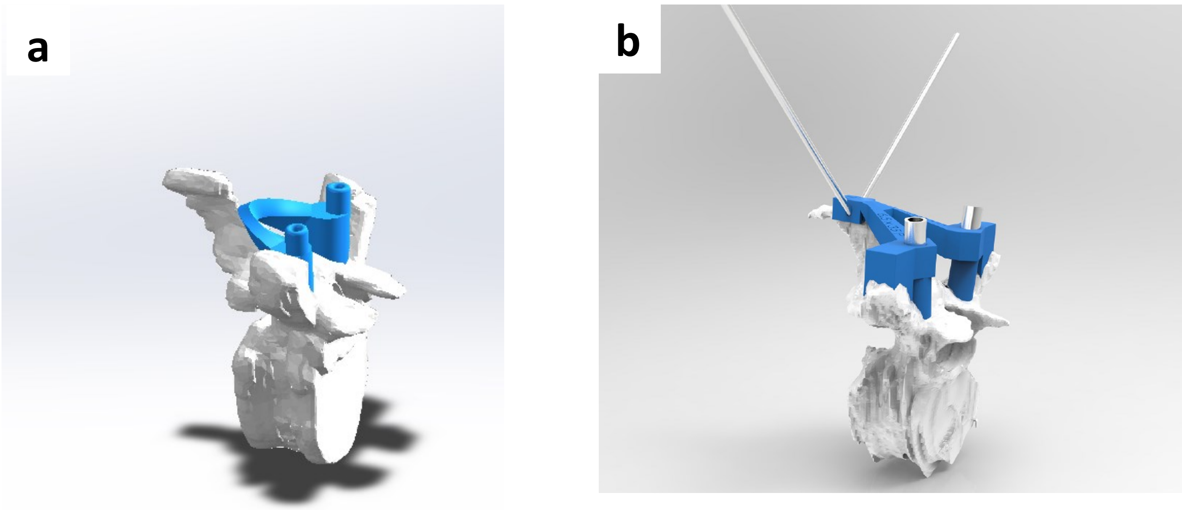

Figure 2 - a) SpineGuide developed by Swaan in 2012 with support blocks on laminae and superior spinous process and b) SpineGuide developed by Drost in 2017 with support blocks on laminae, transverse processes and extremity of the spinous process [25,29].

1.3 MEDICAL BACKGROUND

1.3.1 Anatomy of the spinal column

The spinal column is made of bones, nerves, muscles, and ligaments. The vertebrae are the building blocks of the spine. There are 24 individual vertebrae divided in 7 cervical, 12 thoracic and 5 lumbar vertebrae, figure 4b. The sacrum and the coccyx consist of fused vertebrae, 5 and 4 respectively. A vertebra consists of the vertebral body anteriorly and the pedicles, lamina, and processes (vertebral arch) posteriorly. Together they surround and protect the fragile spinal canal. Vertebral bodies are separated by a cartilage disc, the intervertebral disc, which allows flexibility and prevents bone-bone contact. The vertebral arches are linked by facet joints. Several ligaments connect the vertebrae and provide stability and stiffness. The outer layer of a vertebra, the cortical layer, consist of compact bone and very strong. The inner layer, the cancellous bone, consists of spongy bone which is very light and well perfused. The size and shape of the vertebrae are dependent on the placement in the spinal column, influenced by weight, posture and local flexibility. Therefore, cervical vertebrae are smaller in size than lumbar vertebrae, and their facet joints are differently orientated.

1.3.2 Scoliosis and surgery

Scoliosis is a three-dimensional deformity of the spinal column characterized by lateral displacement and axial rotation of the vertebrae, figure 3. Scoliosis is distinguished in two groups; idiopathic scoliosis (80-90%) and non-idiopathic scoliosis (10-20%). Several conditions can cause non-idiopathic scoliosis, such as congenital abnormalities, neuromuscular disorders and mesenchymal disorders [30]. Idiopathic scoliosis, as the name states, has an unknown underlying cause and is divided into three subgroups; infantile (1%), juvenile (10-15%) and adolescent (±90%). The prevalence and severity of scoliosis are higher in girls than in boys.

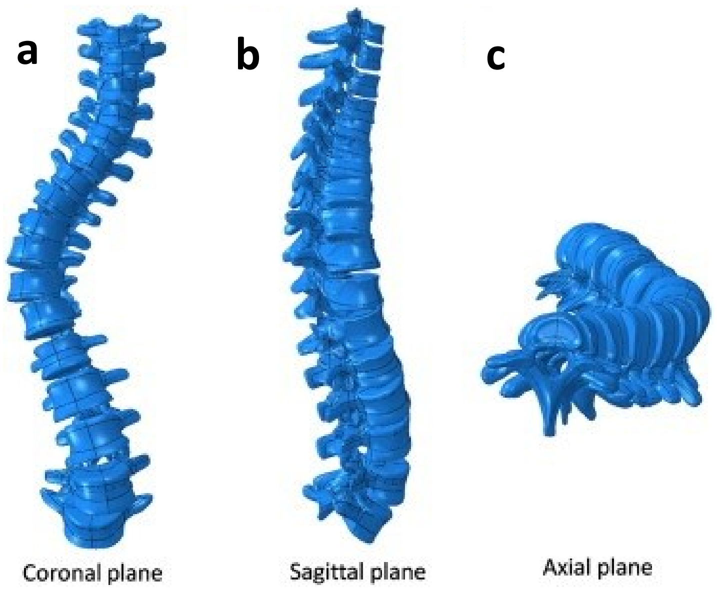

Figure 3 – A visualization of a scoliotic spine in three planes: a) coronal, b) sagittal and c) axial. In the axial plane, the rotation of the vertebrae is well shown [31].

In spite of the fact that scoliosis is a three-dimensional deformity, it is graded by measuring the Cobb's angle of the scoliotic curve in posterior-anterior X-ray, figure 4a. Scoliosis is diagnosed when the Cobb's angle is ≥10° [32]. Orthopaedic surgeons mainly rely on Cobb's angle measurements to follow up the development of scoliosis. Cobb's angle ≥45° are known for their progression after full spinal development and need surgical intervention.

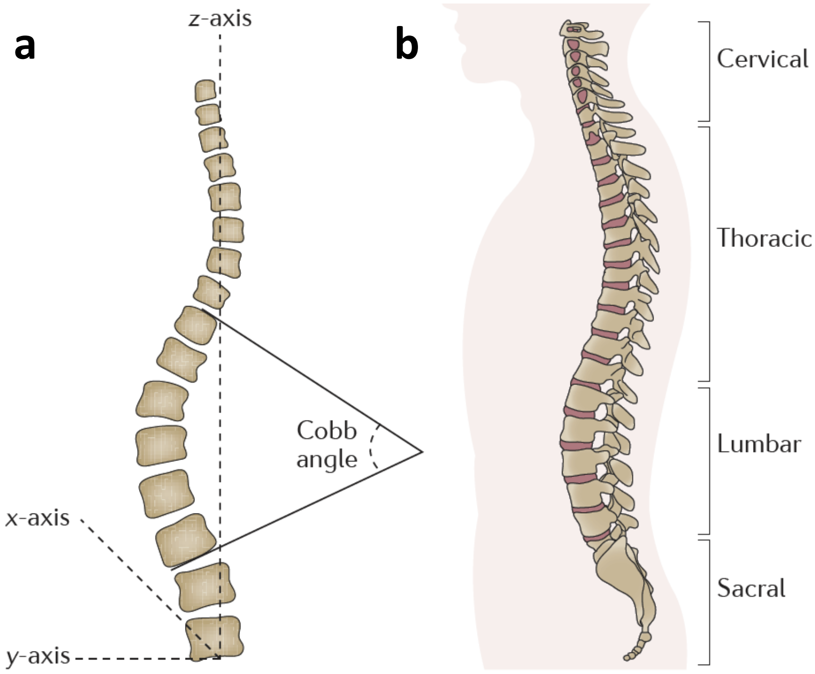

Figure 4 – a) The Cobb's angle is measured in the coronal plane using a posterior-anterior X-ray by drawing a line parallel to the superior endplate of the most tilted upper vertebrae and a line parallel to the inferior endplate of the most tilted lower vertebrae. b) The spinal column divided into four regions in a sagittal view. Figures adapted and adjusted from Cheng et al. 2015 [32]*.*

Progressive curves have a severe and irreversible effect on pulmonary and cardiac function [33,34]. Spinal arthrodesis, or fusion, is the primary goal of surgery to prevent these long-term consequences of deformities of the spinal column and thorax [32]. Thereby, restoring spinal alignment and reducing the deformities are secondary goals of surgery. Hooks, wires, and pedicle screws are used during scoliosis surgery to form 'anchors' to the bony parts of the vertebra, figure 5b. Then, 3D corrective forces are applied to these anchors after which longitudinal metal rods are connected to the anchors to provide correction and stabilization. Especially the preparation and insertion of a pedicle screw is a challenging task in which the surgeon free-handedly makes a hole through the pedicle and vertebral body. Accurate positioning of the screws is essential to gain optimal strength and to prevent damage to the spinal canal, lungs, nerve roots and vessels. Vertebrae in a scoliotic spine can be dysplastic, which makes insertion even more challenging. Liljenqvist et al. show that scoliosis is associated with intravertebral deformities and smaller pedicles on the concave side [35]. The use of the SpineGuide could increase the accuracy of pedicle screw insertion and, thereby, the safety of the patient. In recent literature, several groups report the use of patient-specific drill guides for placement of pedicle screws [4–19].

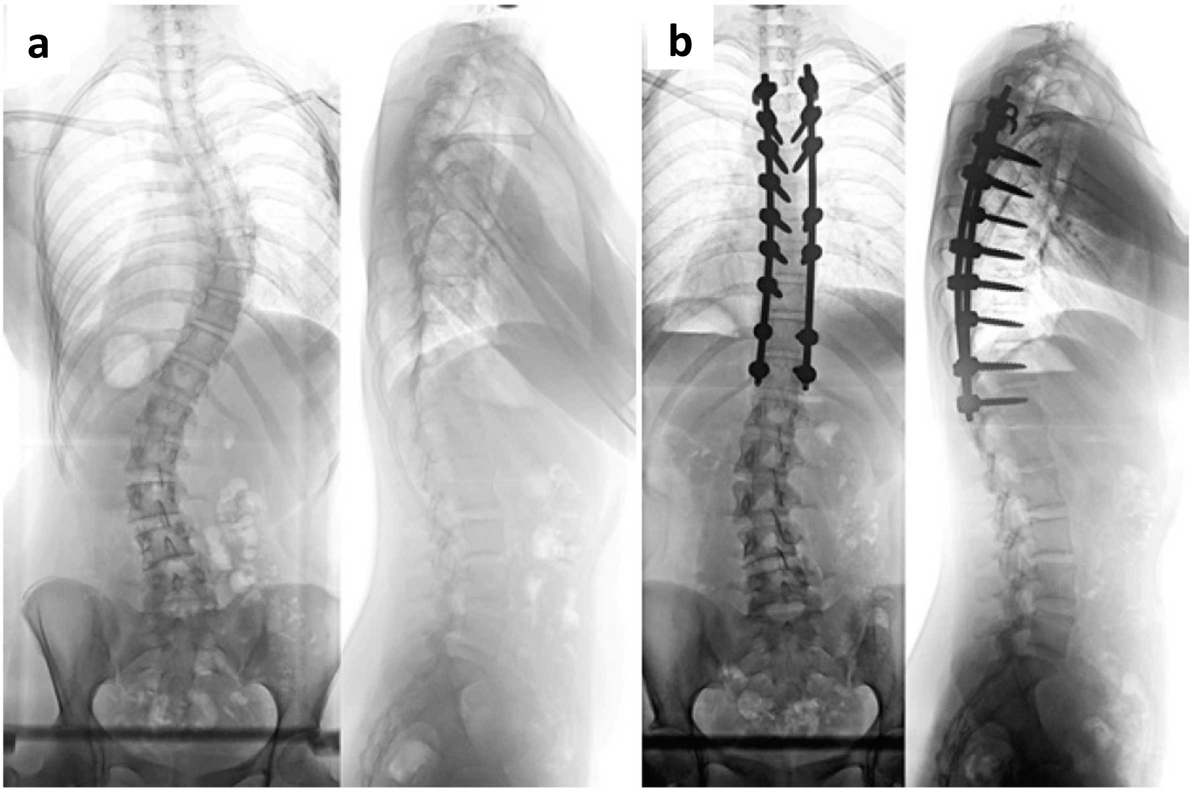

Figure 5 – a) Posterior-anterior and lateral X-ray of a scoliosis patient before surgery and b) posterior-anterior and lateral X-ray of a scoliosis patient after scoliosis correction surgery with two longitudinal rods and pedicle screws and hooks as anchors. X-rays are adapted from Cheng et al. 2016 [32].

1.3.3 Vertebral derotation

Since the beginning of the 1990s surgeons start using pedicle screws in lumbar and thoracolumbar vertebrae in lower end spinal deformity constructs [36]. These screws proved superior to hook constructs. The success of the pedicle screw led to increased use by scoliosis surgeons in the thoracic spine. Advantages of pedicle screws are a secure 3-column fixation, superior control of the upper and lower instrumented vertebrae, and better control of larger scoliosis deformities with posterior instrumentation. With the advent of pedicle screws, scoliosis surgeons became aware of not only treating the coronal correction, but also the axial (apical) vertebral rotation. Intraoperatively surgeons use two maneuvers to correct spinal deformities; direct vertebral body derotation (DVBD) and rod derotation. In rod derotation, the surgeon instruments the rod and then turns the rod for sagittal, coronal and axial correction. DVBD was developed to improve axial rotational correction rate. Pratt et al. described in the early 2000s the use of sticks attached to pedicle screws for apical vertebra rotation [37]. Lee et al. described the clinical application of DVBD and reported 42.5% apical vertebral rotation compared to 2.4% by rod rotation maneuver [38]. Fu et al. showed more effectively corrected vertebral rotation in AIS with posterior pedicle screw constructs, compared to the use of hooks and wires [39]. They used a rod rotation maneuver. They suggested this may be due to the possibility of applying force on a point farther away from the rotational axis of the vertebra. Asghar et al. showed similar results with the DVBD technique used in all pedicle screw constructs compared to hooks and wire constructs, 60% versus 22% respectively [40]. Thereby, they showed a lessened rib prominence associated with vertebral body derotation. Hwang et al. and Chang & Lenke compared different DVBD devices and techniques and proved their effectiveness in the correction of (apical) vertebral rotation and rib prominence [36,41]. However, Hwang et al. mentioned the increased blood loss, operation duration, and volume of blood transfusion using these BVBD techniques. Rushton and Grevitt reviewed the effectiveness of DVBD techniques in scoliosis [42]. They concluded that there is little evidence for using derotation techniques compared to conventional techniques. The studies they reviewed reported between 37 and 63% derotation of the apical vertebra rotation compared to the sagittal plane measured on CT. However, it is unclear if the derotation is simply related to improved coronal and translational correction instead of the derotation techniques. Some of their reviewed studies mentioned rib hump correction as well. The techniques may improve radiographic measures, but do not improve correction of rib hump or quality of life. So the techniques failed to demonstrate to benefit in rib hump correction. We want to explore the use of extreme positioned pedicle screw and their aid in vertebral derotation.

1.4 TECHNICAL BACKGROUND

1.4.1 Biomechanics of axial derotation

In axial derotation techniques a rotational torque is applied to pedicle screws. The torque is translated to force on the vertebral bodies to obtain rotational correction in the axial plane. Gregerson and Lucas demonstrated that the axial rotation of the spine is an integral part of lateral bending in the thoracolumbar spine [43]. In scoliosis correction surgery, when the spinal segments are rotated, lateral bending of the spine also occurs. This phenomenon is referred to as "coupled motion of the spine" [44,45]. In DVBD the axial rotation is translated into a more anatomical true three-dimensional correction [46].

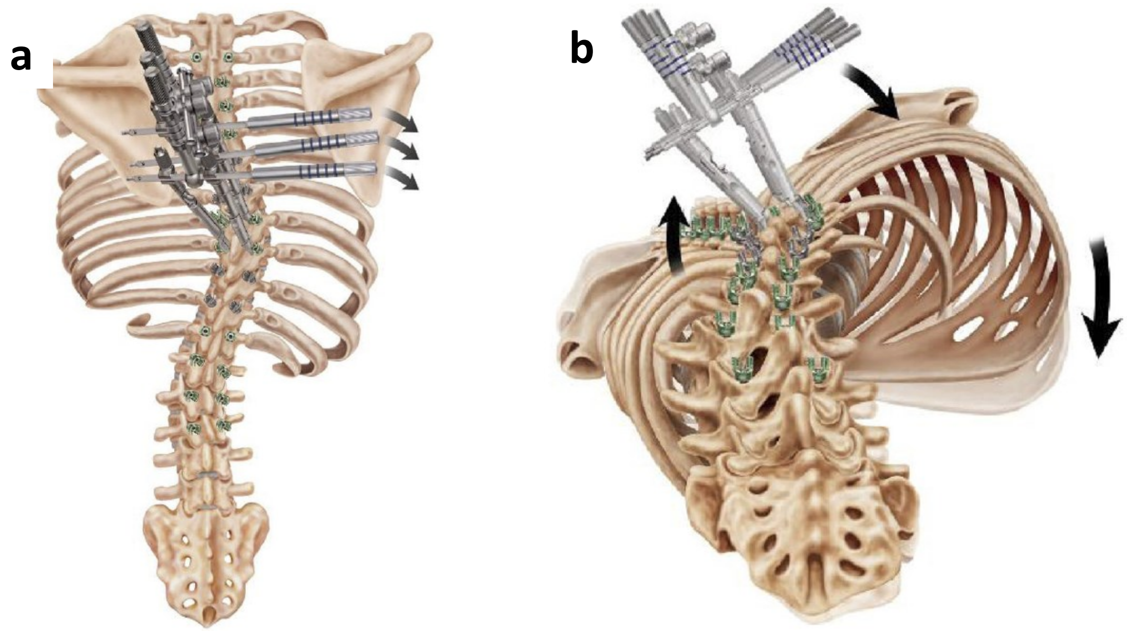

Figure 6 – a) Posterior view of DVBD in scoliosis surgery using specialized instrumentation with derotator tubes and b) axial view of the DVBD technique. Figures are adapted from Chang and Lenke [36].

Fu et al. suggested that by applying a force to a point farther away from the rotational axis of the vertebra, more rotation should be achieved [39]. In DVBD this is done by long tube derotators attached to the pedicle screws, figure 6. In the case of extreme screw positioning the lateralization of the screw head gives the advantage of a point farther away from the rotational axis of the vertebra. Thereby, this point can be even farther by creating a large offset between pedicle screw head and instrumentation rod. This can be done by pre-bending the rod up to 27mm offset (limited by deformity reduction jacket dimension). Interaction is expected between the stiffness of the rod and the stiffness of the spine resulting in a rotated vertebra. The screw and vertebra will be pulled towards the rod in the first stadium of fitting the rod in the screw head, figure 7. In a second stadium, the rod will deform plastically because of high forces and the screw will not be pulled any further towards the rod. Around 800 newton is needed to plastically deform a Cobalt-Chrome (CoCr) 5.5 mm rod [47]. A downside of loading the screws in the axial plane (medial or lateral) is breakout of the pedicle screws. Bianco and Aubin stated that nonaxial loads on pedicle induce screw plowing that leads to bone compacting and subsequent screw loosening or even bone failure [48].

The forces can be determined by several methods, for instance these two:

1. During fitting the rod in the screw head, torque can be measured using a torque wrench. The torque is measured on a cricket. The torque can be translated in the force applied to the rod and screw and may give insights in the biomechanics of vertebral derotation.
2. Calculating the force on the screw and rod by Finite Element Modeling (FEM). In FEM the material characteristics of CoCr rods and the changing geometry of the rod between different time points can be used to simulate the forces acting on the rod [47].

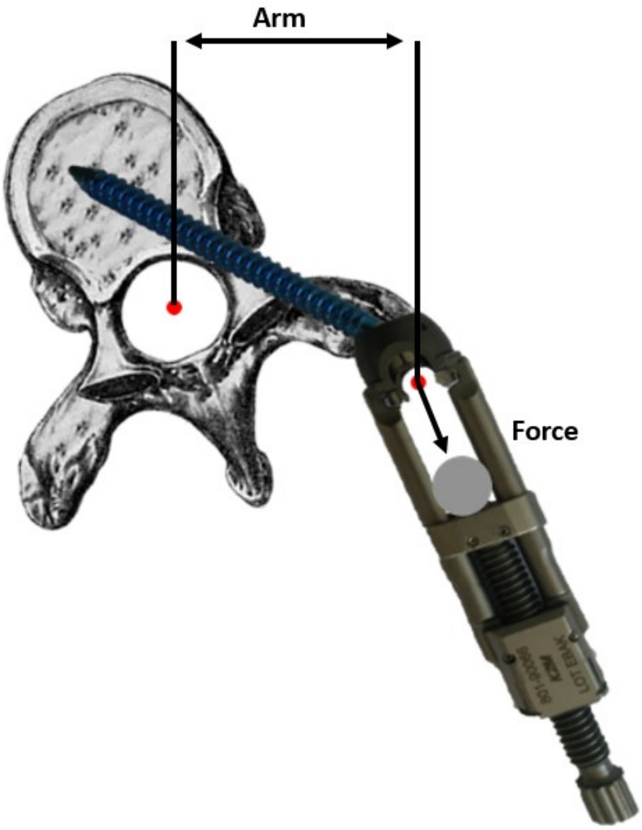

Figure 7 – An extreme positioned pedicle screw and the cricket. The extreme screw trajectory has a longer arm and following the equation torque = F x A, the torque is easier translated to a force for rotation of the vertebra. The exact position of the vertebral rotation point, especially with instrumentation, is under discussion. However, the arm will always be longer independently where the rotation point exactly is.

1.5 THESIS OUTLINE

We believe that extreme pedicle screw positioning has the potential to aid in the axial vertebral derotation in scoliosis surgery, because it increases the moment arm, and hence with the same force, a higher moment of force (torque) can be generated. For this reason, the main goal of this study was to determine what the most extreme pedicle screw position is, given the maximal polyaxial angle (30°) of the K2M Mesa screw and the work length of the deformity reduction jacket (cricket, 27mm). To achieve this goal, a biomechanical cadaver spine model will be used, and we are interested in:

- Possibility to produce this extreme screw position in a cadaver vertebra using the SpineGuide.
- Influence of extreme screw position on the axial vertebral rotation of the instrumented vertebra.
- Distribution of force on the extreme pedicle screw towards axial vertebral rotation.
- Accuracy of pedicle screw placement using the SpineGuide.

Based upon biomechanics, we hypothesize that the amount of rotation of a vertebra increases by an increased offset between pedicle screw head and the rod, and a point further away from the rotational axis of the vertebra. Thereby, the manufacturing process and stability of the SpineGuide have room for improvement and, secondly, the accuracy of the use of the SpineGuide should be measured and validated.

2 MATERIALS AND METHODS

2.1 STUDY OVERVIEW

A study overview is given in flowchart 1. The study was a feasibility study in a human cadaver spine. We instrumented short spine sections (three vertebrae and two discs) with an extreme positioned screw in the middle vertebra. Screw positioning was realized with the aid of the 3D printed SpineGuide based on boneMRI. We used a straight rod on the contralateral side and a pre-bent rod on the extreme screw side. The extreme positioned screw was then pulled towards the rod, with simultaneously a torque measurement. A CT scan was made afterward to measure rotation and translation of the relevant vertebra, and for determining rod deformation.

The boneMRI was used to delineate the vertebrae for volume rendering in MeVisLab. Conventional and extreme pedicle screw trajectories were planned in the vertebrae volumes in SolidWorks. The segmentations including the planned trajectories were used to manufacture the SpineGuide in SolidWorks, based on the vertebral anatomy.

2.2 MATERIAL COLLECTION & PREPARATION

2.2.1 Specimen

One fresh-frozen human cadaver (non-scoliotic) spine, female age 57, was used for the feasibility study. The specimen consisted of the spine, posterior rib cage, pelvis, and part of the femur. Bone mineral density of the specimen was not measured. All soft tissues attached to the spinal column were left untouched to approximate the in vivo stiffness and flexibility as much as possible.

2.2.2 Medical image acquisition

Medical images of the specimen were obtained. A CT was made to check for abnormalities in the spine. Then, a boneMRI was made to visualize cortical bone in MRI.

2.2.3 Manufacturing SpineGuide

The medical imaging processing and visualization software MeVisLab was used for manual segmentation of a total of 13 vertebrae (T3-L3) and the spinal canal [49]. Each vertebra was manually segmented using spline interpolations in the boneMRI data. The delineations were done in the axial slices of boneMRI, resulting in volume composed of slices. Then, the volume was converted to a 3D mesh of polygons ('.stl-file') with high accuracy settings. Vertebrae were individually segmented and saved. The network used in MeVisLab can be found in Appendix 7.1.

Once the vertebrae (T3-L3) and spinal canal were delineated by hand, the volumes were exported to the SolidWorks Student Edition, a 3D computer-aided designer software [50]. In SolidWorks the spinal canal was cut out of the vertebrae, so pedicle dimensions were visible. After that, in case of a conventional pedicle screw, trajectories were planned unicortical, as shown in figure 1a. In case of an extreme positioned pedicle screw, the trajectory was allowed to be in-out-in/tricortical, as shown in figure 1b. Only the middle vertebra of a spine segment was instrumented with an extreme positioned screw on one side. The planned trajectories were checked by an experienced orthopaedic scoliosis surgeon (M.K.). The steps executed in SolidWorks can be found in Appendix 7.2.

Finally, a new version of the SpineGuide was designed in SolidWorks. The SpineGuide consists of five contact points matching the anatomy of the vertebrae, figure 9a. A support block guiding the drill

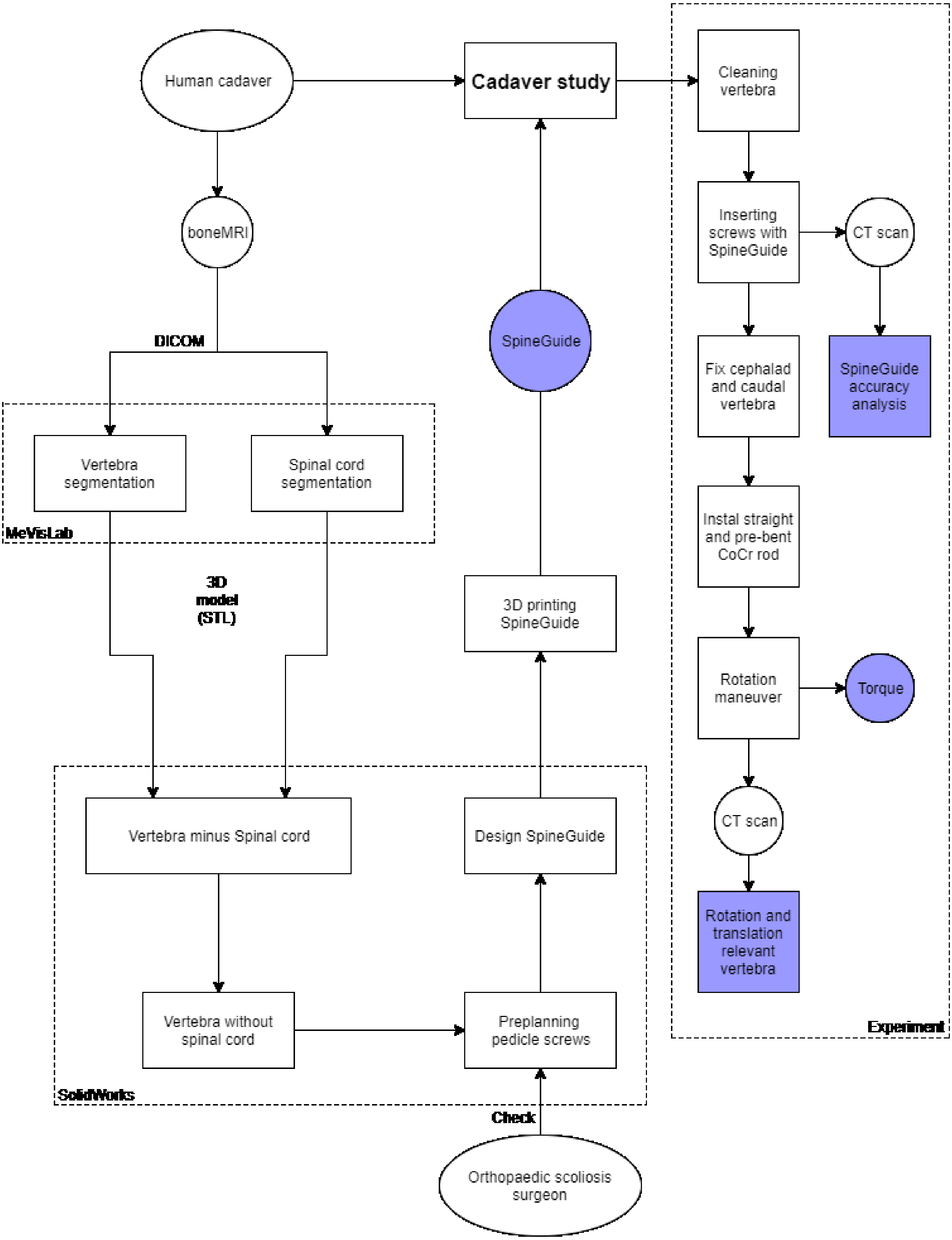

Flowchart 1 – An overview of the study with the steps performed in MeVisLab and SolidWorks to manufacture the SpineGuide. Thereby, the steps performed during the experiment and the outcome variables in the blue blocks.

trajectory to the lamina (right and left), a support block on the transverse process (right and left) and a support block on the spinous process. Thereby, two holes in the spinous process support block were designed to attach the SpineGuide to vertebrae with k-wires for a stable fit, figure 8a. The designed SpineGuides were send to a 3D printing company (Oceanz, Amersfoort, The Netherlands [51]) for additive manufacturing in PA2200 nylon material. The SpineGuide fit was verified using a 3D printed model of the vertebra, figure 8b. Metal drill bushings were manufactured to be inserted into the SpineGuide to protect the nylon during drilling. Designing steps of the SpineGuide can be found in the Appendix 7.3.

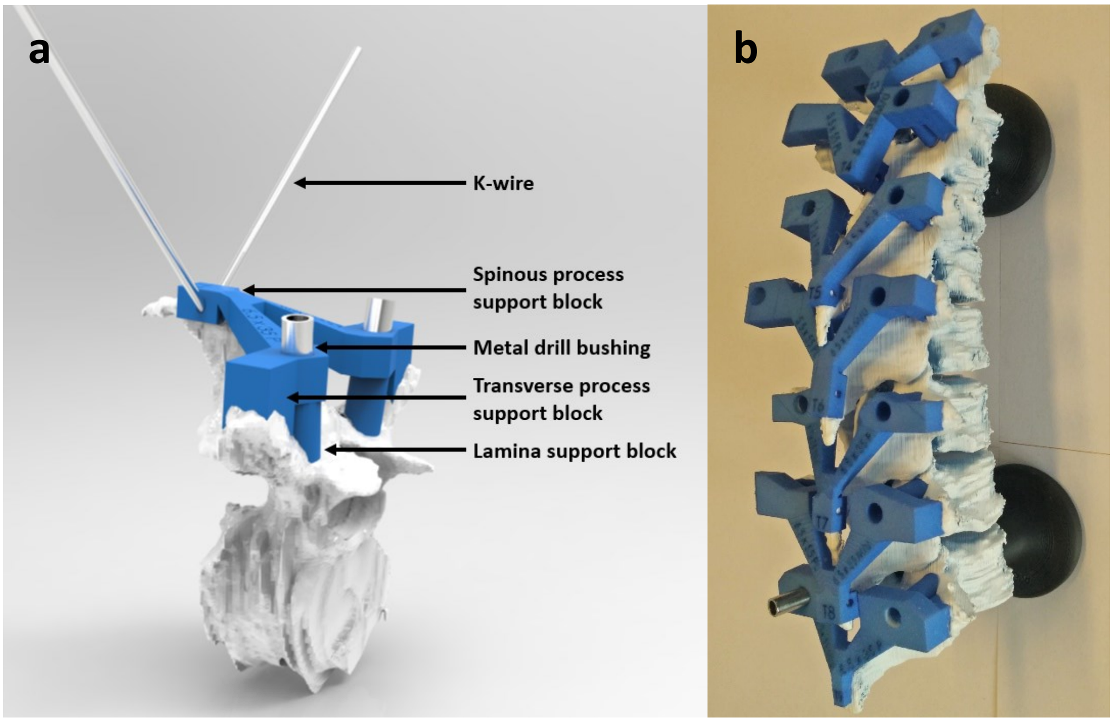

Figure 8 – a) The new version of the SpineGuide and all its parts and b) the verification test of the 3D printed SpineGuides on the 3D printed model of the vertebrae.

2.2.4 Spinal instrumentation

In this study, the MESA deformity spinal system by K2M was used [52]. The system consists of 5.5mm CoCr rods fitting into pedicle screws. The diameter of the pedicle screws used were 5.5mm and 6.5mm uniaxial and polyaxial, differing in length (35 – 55 mm). The distribution of the screws is visualized in figure 10c. Deformity reduction jackets (crickets) were used to accomplish correction maneuvers in all planes. Lock instrumentation tools were used to lock the pedicle screw heads.

2.2.5 Calibration cricket

We determined the forces via two methods as explained in paragraph 1.4.1. A calibration of the cricket was performed to establish translation of the torque (Nm) needed to lift a known weight (Kg). A calibration curve was created by extrapolating the results to find the relationship between torque (Nm) and force (N), Appendix 7.4. In this way, we were able to translate torque needed to fit the rod into the pedicle screw head to the force acting on the rod and screw. Alternatively, the forces acting on the screws were computed by simulating the deformation of the rods in a FEM simulation [47]. The outcomes of the FEM simulations were used to compare with the torque measured in the cadaver study. The outcome and methods of the FEM simulations can be found in Appendix 7.5.

2.3 CADAVERIC FEASIBILITY STUDY

2.3.1 Screw placement

The specimen was opened by a posterior mid-line incision and lamina, transverse processes and spinous process were cleaned as in a standard scoliosis surgery procedure. The facet joints were left intact. Then, the fit of the SpineGuide was validated on the cleaned vertebra. Additional cleaning was performed in case of incorrect fit. The SpineGuide was placed on the matching vertebra and was attached to the spinous process with K-wires, figure 9a and 9b. After that, a 3.8mm drill bit was used to drill the hole through the pedicle, figure 9c. When the trajectories were drilled, the SpineGuide was removed, the trajectories were checked for a cortical breakout by palpating the hole and the pedicle screws were inserted. All steps were repeated for the 13 vertebrae and performed by an experienced orthopedic scoliosis surgeon (M.K).

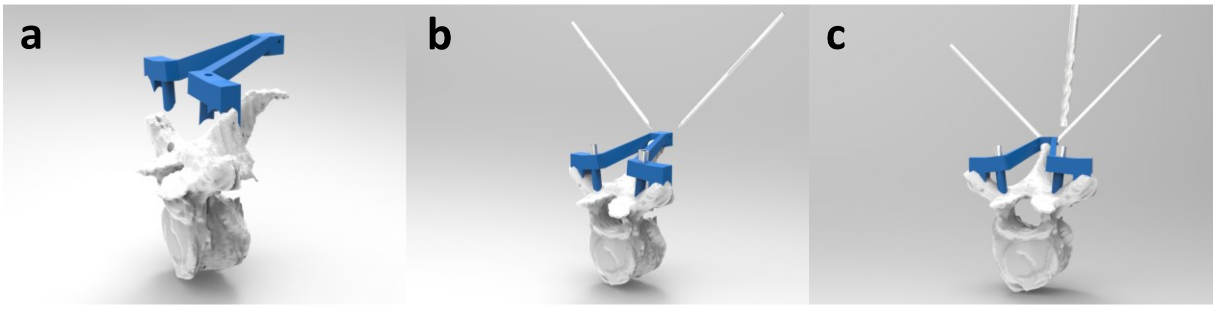

Figure 9 – a) The SpineGuide placed on the vertebra, b) the K-wires inserted in the spinous process through the spinous process support block and c) drilling through the SpineGuide using a 3.8 mm drill bit.

2.3.2 Experimental setup for derotation

The experimental setup was prepared after drilling and inserting the pedicle screws. The 13 vertebrae were subdivided into six short spine sections (three vertebrae and two discs) for testing as shown in figure 11a and 11b; T3-T5, T5-T7, T7-T9, T9-T11, T11-L1, and L1-L3. In each segment of three vertebrae, the left pedicle screw of the middle vertebra was an extreme positioned one. The adjacent vertebrae (cephalad and caudal) were fixed to a wooden beam using plastic bolts and nuts to prevent rotation and translation. The middle vertebra was unfixed and constrained by ligamentous attachments (cephalad and caudal intervertebral discs and superior and inferior facets).

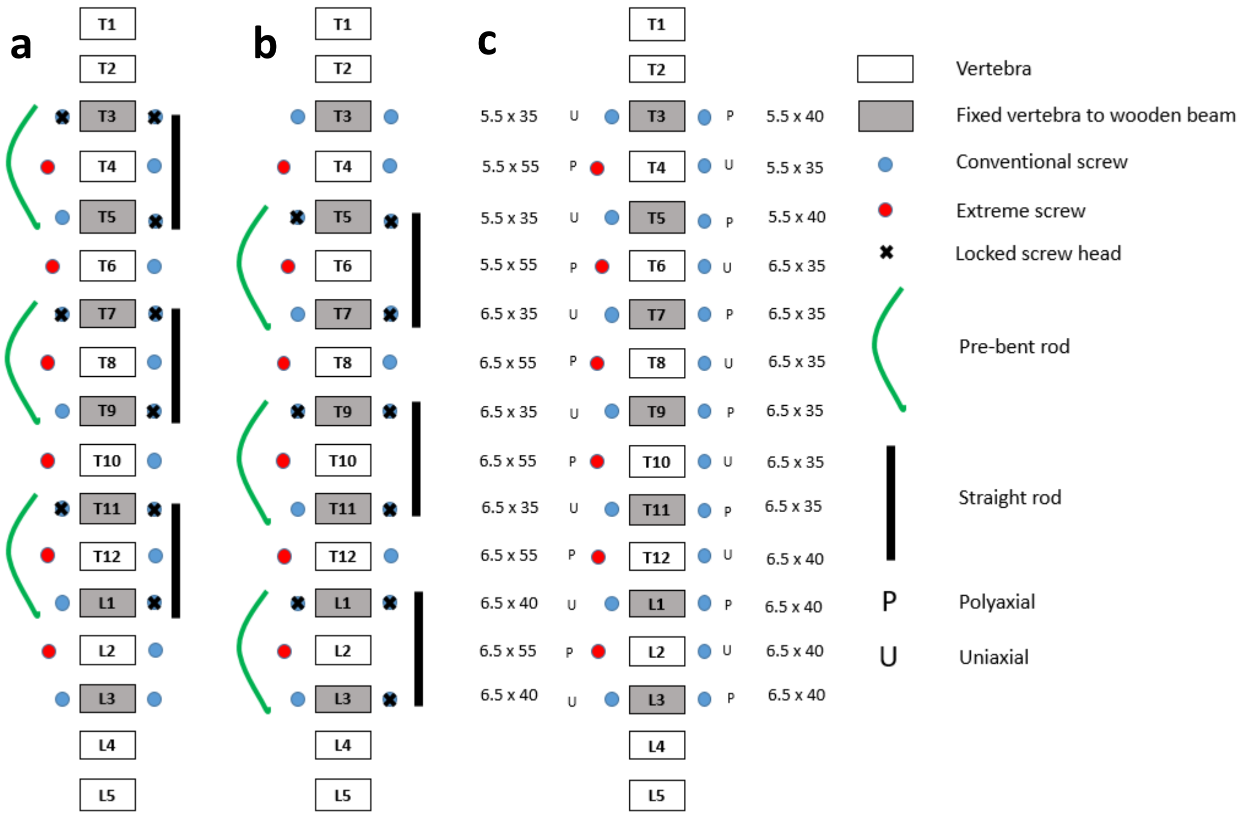

Figure 10 – a) Experimental setup as in measurement set 1 (T3-T5, T7-T9, T11-T12), b) experimental setup as in measurement set 2 (T5-T7, T9-T11, L1-L3) and c) distribution of the pedicle screws with their diameter x length in mm and type of screw head.

2.3.3 Axial derotation maneuver with extreme screw positioning

Measurements of axial derotation were performed at two time points using two measurement sets. The short spine segments T3-T5, T7-T9 and T11-L1 are the first measurement set, and the short spine segments T5-T7, T9-T11 and L1-L3 the second measurement set, figure 10a and 10b. Spinal rod instrumentation was implanted in the following steps for the first measurement set, figure 11a and b:

- First T3-T5, then T7-T9 and at last T11-L1:
  1. On the contralateral (right) side a straight 5.5mm CoCr rod was attached to the pedicle screws (cephalad, middle and caudal) and the cephalad en caudal screw head were locked.
     - A cricket was used to prevent the rod from major movements out of the middle screw head.
  2. On the left side a pre-bent rod was attached to the cephalad and caudal pedicle screw head of each segment and only the cephalad screw head was locked;
     - The rod was pre-bent beforehand to a maximum curve offset of 27 mm.
     - A cricket was used to prevent the rod from major movements out of the caudal screw head.
  3. The cricket was used to fit the rod into the middle pedicle screw head;
     - Force acting on the rod and middle screw was measured using a torque wrench. The torque wrench was attached to the cricket and after each quarter turn, the torque was noted. This was done until the rod fit into the pedicle screw head.
  4. All pedicle screw heads were locked with the lock instrumentation tools.

Spinal rod instrumentation was implanted in the following steps for the second measurement set, figure 11 c and d:

- First T5-T7, then T9-T11 and at last L1-L3:
    1. On the contralateral (right) side a straight 5.5mm CoCr rod was attached to the pedicle screws (cephalad and caudal) and the screw heads were locked;
        - The middle contralateral pedicle screw had been removed.
    2. On the left side a pre-bent rod was attached to the cephalad and caudal pedicle screw head of each segment and only the cephalad screw head was locked;
        - The rod was pre-bent beforehand to a maximum curve offset of 27 mm.
        - A cricket was used to prevent the rod from major movements out of the caudal screw head.
    3. The cricket was used to fit the rod into the middle pedicle screw head;
        - Force acting on the rod and middle screw was measured using a torque wrench. The torque wrench was attached to the cricket and after each quarter turn, the torque was noted. This was done until the rod fit into the pedicle screw head.
    4. All pedicle screw heads were locked with the lock instrumentation tools.

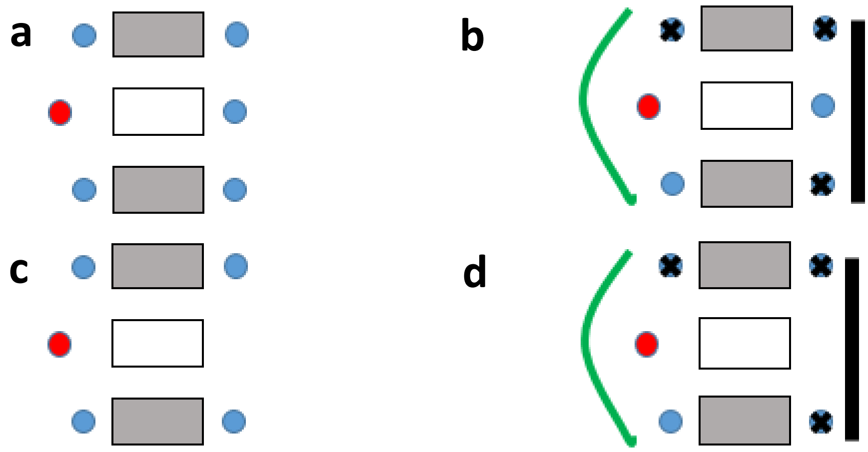

Figure 11 – a) and b) Schematic visualization of short spine segment with an extreme positioned pedicle screw (red) on one side in the middle vertebra as in measurement set 1. A straight rod (black) is instrumented on the contralateral side and the pre-bent rod (green) on the other side. The pre-bent rod is instrumented with an offset between the center of the rod and the extreme pedicle screw head. c) and d) Schematic visualization of short spine segment as in measurement set 2 with the middle screw on the contralateral side removed.

2.3.4 CT acquisitions

CT scans were made at four time points of the study to obtain information about the drill accuracy and the rotational and translation movement of the vertebrae:

- 1: The pedicle screws on all levels are inserted in the spine and cephalad and caudal vertebrae are fixed to the wooden beam.
    - To determine pedicle screws placement accuracy.
    - To determine baseline positions vertebrae.
- 2: The specimen with the rods instrumented as in measurement set 1 after final locking.
    - To determine rotational and translation movement of the relevant vertebrae.
- 3: The specimen with the rods instrumented as in measurement set 2 after final locking.
    - To determine rotational and translation movement of the relevant vertebrae.
- 4: The specimen without the pedicle screws and fixation materials.
    - To determine screw hole accuracy and (if different) drill hole accuracy.

2.4 ANALYSIS

2.4.1 SpineGuide accuracy

An experienced surgeon assessed the placement of the pedicle screws following Neo's classification (grade 0: no perforation; grade 1: perforation <2 mm; grade 2: perforation ≥2 mm but <4 mm; grade 3: perforation ≥4 mm) [53]. The accuracy of the SpineGuide was determined using the CT of time point 1 with pedicle screws inserted. Each vertebra in the CT was matched by hand on the corresponding vertebra of the pre-experimental boneMRI using MeVisLab, so coordinates of the CT are in the same world frame as the MRI. Then, in the matched CT the pedicle screws were segmented using a region growing segmentation algorithm in MeVisLab. After that, the segmented pedicle screws were exported to SolidWorks and visualized together with the vertebra with the preplanned trajectories. In SolidWorks, entry point deviation between segmented pedicle screws and preplanned trajectories was measured, as well as the angular deviation. The mean and standard deviation (SD) of the entry point and the angle were calculated using Microsoft Excel (2013) [54]. Steps executed can be found in Appendix 7.6.

2.4.2 Axial derotation maneuver with extreme positioned pedicle screw

The axial rotation and translation of the vertebra were determined in MeVisLab by comparing the CT of time point 1 with the CT of time point 2 in case of measurement set 1 and by comparing the CT of time point 1 with the CT of time point 3 in case of measurement set 2. The CT of time point 1 was the reference image and for each short spine segment the CT of time point 2 or 3 was matched by hand, so both CTs were in the same world frame. Registration was done by matching the cephalad and caudal fixed vertebrae of each short spine segment. Afterwards, five identifiable anatomical points were indicated in the middle vertebra in both CTs, figure 12. The coordinates of these anatomical points were used to determine the orientation of the middle vertebra at baseline and after instrumentation. MATLAB (2015) was used to determine the axial rotation accomplished by the instrumentation maneuver with extreme positioned pedicle screws [55].

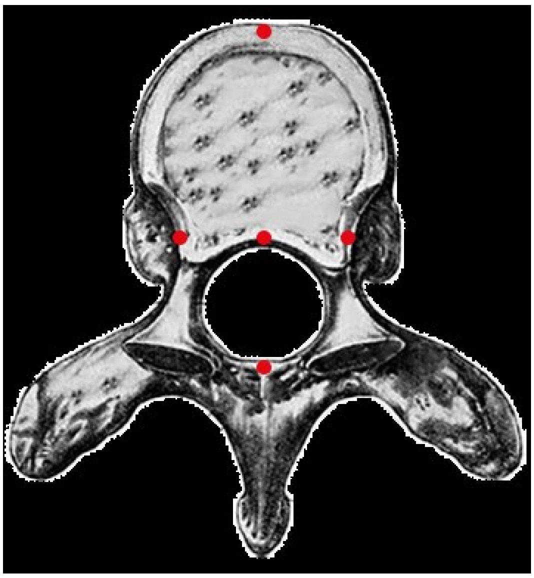

Figure 12 – The five anatomical points used for determining the orientation of the middle vertebra at baseline position and after the rotation maneuver. The axial rotation between the coordinates of these five points in two time points is calculated using MATLAB (2015).

3 RESULTS

3.1 SPINEGUIDE ACCURACY

In total 13 SpineGuides were manufactured and used for drilling (T3-L3), figure 13a. The T6, T9 and L3 SpineGuide had an unstable fit during verification on the 3D printed vertebrae model. The T9 and L3 SpineGuide were able to tilt on the specimens vertebra. Furthermore, the T6 SpineGuide touched the spinous process of T5 and the spinous process of T3 and T4 were damaged due to unknown cause. All SpineGuides were used despite knowing these three had an unstable fit.

Of the 13 SpineGuides, 12 were correctly placed on the specimens vertebrae. The T12 SpineGuide was misplaced and therefore excluded from the quantitative results. CT visual assessment by an expert confirmed that of the conventional pedicle screws 11 (57.9%) were fully inside the pedicle of a total of 19 inserted conventional screws, table 1. There were five Grade 1 (26.3%), two Grade 2 (10.5%) and 1 Grade 3 (5.3%) perforations following Neo's classification. The direction of pedicle violation included three medial and three lateral. Two screws penetrated the inferior (Grade 3) or superior (Grade 1) cortex of the pedicle in the sagittal plane. The T5 right screw did not follow the drilled hole and, therefore, the drilled hole was used for accuracy analysis of the SpineGuide instead of the pedicle screw.

Table 1 – A literature overview of studies using patient-specific drill guides for placement of pedicle screws in the thoracic and lumbar spine. All studies used a four grade system to determine the accuracy of the placement of the pedicle screws using patient-specific drill guides. The last row shows the results of the current study.

Papers	**Screws**	**Grade 0 (%)**	**Grade 1 (%)**	**Grade 2 (%)**	**Grade 3 (%)**	**Study type**
Ma et al. 2011 [15]	240	93.3	6.7	0.0	0.0	Cadaveric
Lu et al. 2011 [13]	168	93.5	6.5	0.0	0.0	Clinical
Swaan et al. 2012 [25]	12	91.7	8.3	0.0	0.0	Cadaveric
Merc et al. 2013 [14]	54	89.9	10.1	0.0	0.0	Clinical
Sugawara et al. 2013 [17]	58	100	0.0	0.0	0.0	Clinical
Lamartina et al. 2015 [10]	46	91.3	8.7	0.0	0.0	Cadaveric
Chen et al. 2015 [20]	118	91.5	8.5	0.0	0.0	Clinical
Takemoto et al. 2016 [18]	415	98.4	1.4	0.2	0.0	Clinical
Hu et al. 2016 [5]	582	96.1	3.9	0.0	0.0	Cadaveric
Chen et al. 2016 [21]	50	100	0.0	0.0	0.0	Cadaveric
Farshad et al. 2017 [22]	48	58.3	39.6	2.1	0.0	Cadaveric
Liu et al. 2017 [11]	48	93.8	6.2	0.0	0.0	Clinical
Putzier et al. 2017 [23]	76	84	12.1	3.9	0.0	Clinical
Kong et al. 2017 [9]	29	93.5	6.5	0.0	0.0	Cadaveric
Current study 2017	**19**	**57.9**	**26.3**	**10.5**	**5.3**	**Cadaveric**

Note 1: Farshad, Lamartina and Putzier used Medacta MySpine System [56]*. Lu and Ma operate in the same research group.*

The screw mean entry point deviation of the 19 conventional screws compared with the preplanned trajectory entry point was 2.29 ± 2.42 mm (0.21 mm – 11.87 mm), table 2. The screw mean angle deviation compared with the preplanned trajectory angle was 7.09 ± 4.10˚ (0.58˚ - 14.86˚). We also divided the 19 conventional screws in right and left. The mean entry point deviation of conventional screws on the right and left compared with the preplanned trajectory entry point were 2.53 ± 3.09 mm (0.21 mm – 11.87 mm) and 1.87 ± 0.93 mm (0.92 mm – 3.85 mm) respectively. The screw mean angle deviation of the screws on the right and left compared with the preplanned trajectory angle were 8.81 ± 4.11˚ (3.39˚ - 14.86˚) and 4.14 ± 2.51˚ (0.58˚ - 7.75˚) respectively.

Table 2 – The deviation of the entry points and angle compared to the preplanned trajectories. The mean deviation of all conventional screws, the mean deviation of the conventional screws on the right and the mean deviation of the conventional screws on the left are shown with their standard deviation and minimum and maximum values in brackets. Thereby, the mean deviation of the extreme positioned pedicle screws is shown with its standard deviation and minimum and maximum value in brackets.

	Deviation in mm (range)	Angle in degrees (range)
Mean conventional	2.29 ± 2.42 (0.21 – 11.87)	7.09 ± 4.10 (0.58 - 14.86)
Mean conventional right	2.53 ± 3.09 (0.21 – 11.87)	8.81 ± 4.11 (3.39 - 14.86)
Mean conventional left	1.87 ± 0.93 (0.92 – 3.85)	4.14 ± 2.51 (0.58 - 7.75)
Mean extreme	2.13 ± 1.68 (0.76 - 4.99)	4.62 ± 2.86 (2.76 - 9.42)

Of the proposed six extreme positioned pedicle screws, five were correctly inserted using the SpineGuide. The T12 SpineGuide with extreme screw position was misplaced and therefore excluded from the quantitative results. CT visual assessment by an expert confirmed three medial breaches Grade 1. The extreme positioned screw mean entry point deviation of the five screws compared with the preplanned trajectory entry point was 2.13 ± 1.68 mm (0.76 mm - 4.99 mm). The extreme positioned screw mean angle deviation compared with the preplanned trajectory angle was 4.62 ± 2.86˚ (2.76˚ - 9.42˚).

a b

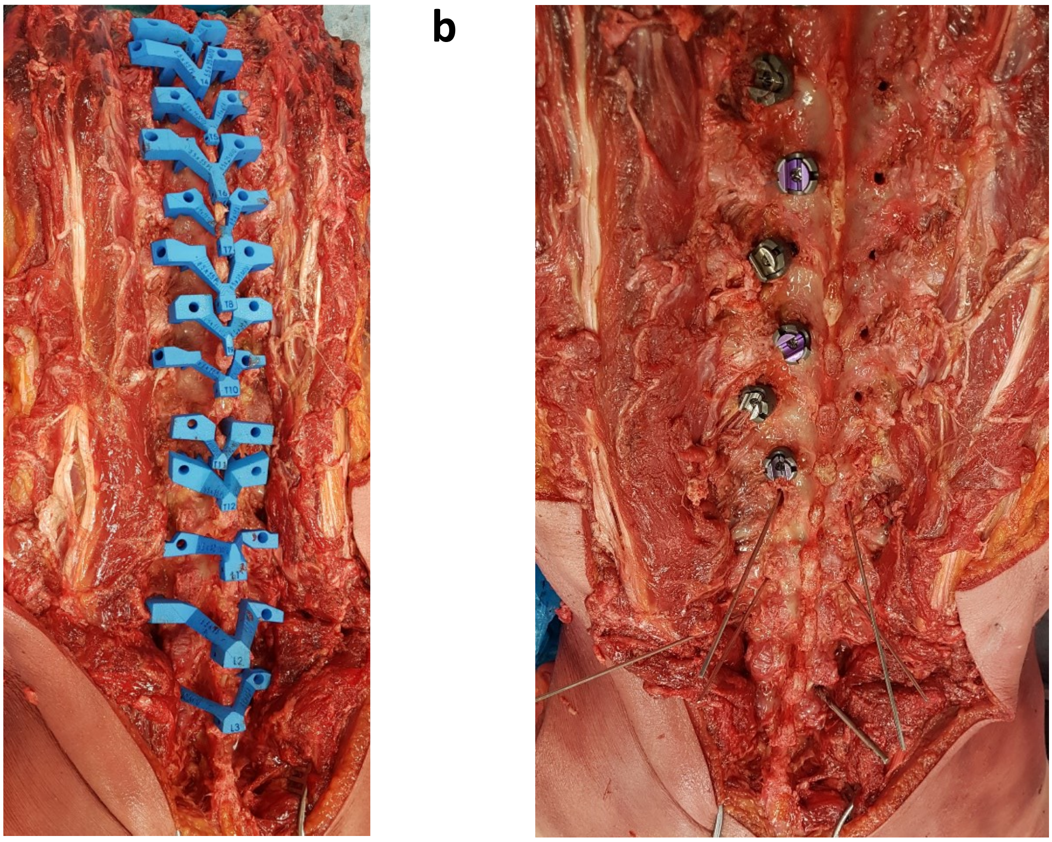

Figure 13 – Two posterior views on the specimens spine with thoracic vertebrae cranial and lumbar vertebrae caudal. a) Validation testing of the SpineGuides on the specimens vertebrae to determine if additional cleaning is needed and b) inserting pedicle screws into the drilled holes and a check of the holes using k-wires.

3.2 AXIAL DEROTATION WITH EXTREME POSITIONED PEDICLE SCREW

As mentioned five of the six extreme positioned pedicle screws were correctly inserted in the vertebrae. The T12 was incorrectly placed. We performed five rotation maneuvers using the pre-bent CoCr rod and the extreme positioned pedicle screws. Four out of five of the pedicle screws broke out during the rotation maneuver (T4, T6, T8, T10) of which two had a visible fracture, table 3. The L2 pedicle screw was still in place after rotation maneuver.

Table 3 – The amount of pull out of the extreme positioned pedicle screws for each segment. Thereby, T4 and T8 had a visible fracture of the transverse process and the medial pedicle respectively.

Vertebra	Fracture	Pull-out
T4	Transverse process	0.5 cm
T6	-	0.6 cm
T8	Medial pedicle	1.2 cm
T10	-	0.5 cm
L2	-	-

During instrumentation, the torque was measured with the torque wrench, Appendix 7.7. The torque values were translated to force using the calibration curve of the cricket, figure 14a and 14b . The force approximated using the torque wrench is visualized together with the force calculated using the FEM simulations of the rod deformation. In T3-T5, T5-T7, T7-T9, and T9-T11 the approximated force is less than the force calculated by the FEM simulation. In L1-L3 the approximated force is higher than the force calculated by the FEM simulation. Finally, the rotation of the relevant vertebra was measured between the baseline position and after the rotation maneuver. In all five measurements, no significant rotation was accomplished (<0.5˚).

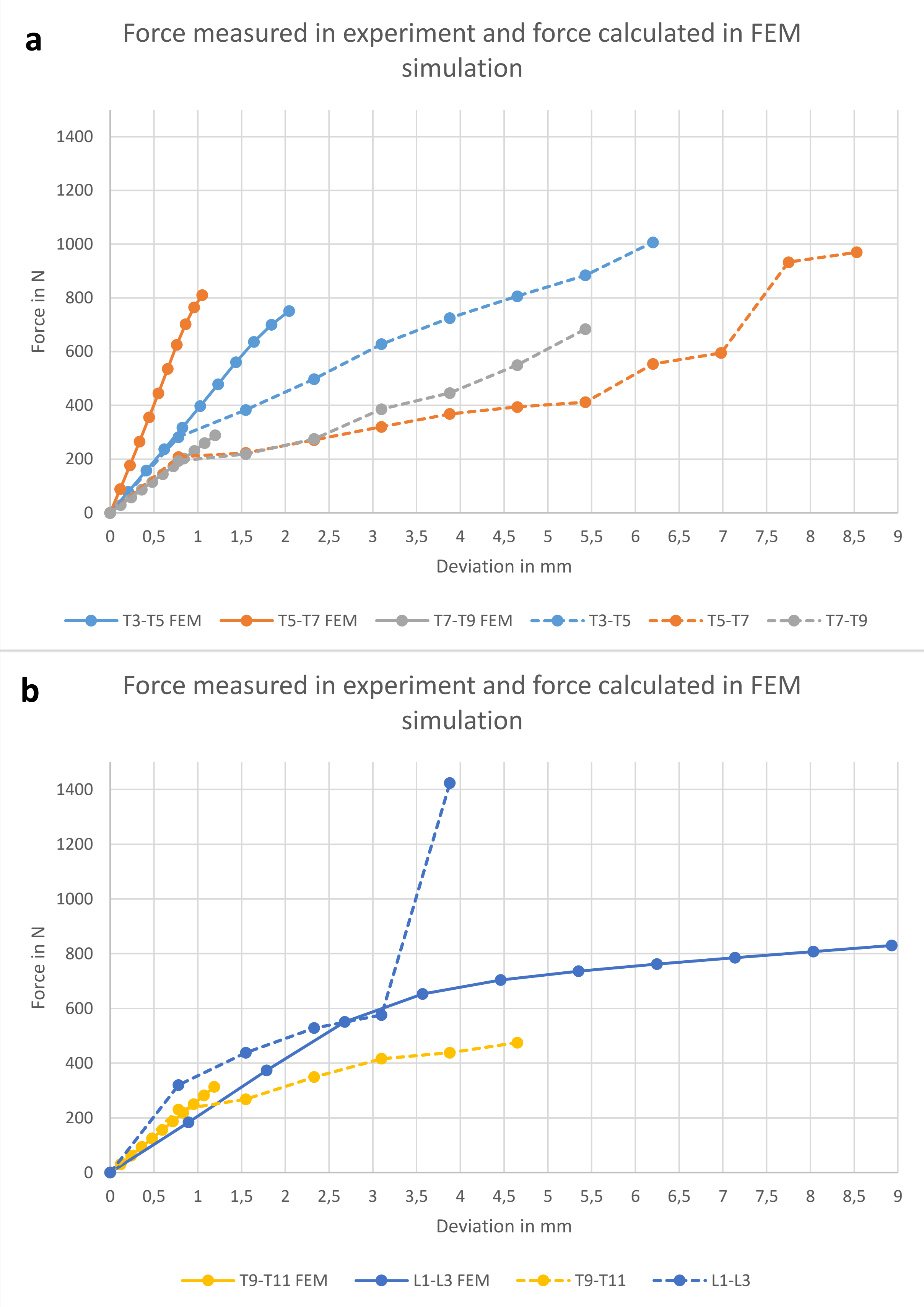

Figure 14 - The forces measured in the experiment using a torque meter for each segment (dotted lines). Thereby, the force calculated using the FEM simulation is visualized as well (solid line). The dotted lines are an approximation of plastic and elastic deformation of the rod. The solid lines are calculation of only plastic deformation of the rod. a) values for T3-T5, T5-T7 and T7-T9, and b) values for T9-T11, L1-L3.

4 DISCUSSION

4.1 SUMMARY

Previous research investigating the use of drill guides for pedicle screw placement described promising results regarding the accuracy and safety [4–19]. However, none of them used the drill guides for extreme pedicle screw trajectories. This study shows that placement of extreme pedicle screws is feasible using the SpineGuide. However, the accuracy analysis of the SpineGuide shows major deviations in entry point and angle compared with the planning. Although the screws could be placed, the reduction force generated with the cricket system caused breakout of most of the extreme pedicle screws. In four of the five rotation maneuvers hardly any rod deformation occurred. This may be a consequence of osteoporotic bone of the specimen. However, the bone density was not measured. Even in the case where the screw was maintained the rotation maneuver using these extreme pedicle screws failed and the rod deformed.

For clinical use of the SpineGuide for pedicle screw placement, the SpineGuide technology should be improved. The SpineGuide may be improved by (1) being more rigid, (2) having only three support blocks, (3) having a superior spinous process support block and (4) being manufactured more automatically. For clinical use of extreme pedicle screws to aid in the vertebral rotation, the cadaveric model should be improved. The model may be improved by (1) using a high bone-density cadaver, (2) fixing the vertebrae more rigidly, (3) using more advanced force measurement tools and (4) using longer spine segments with more 'free' vertebrae.

4.2 SPINEGUIDE ACCURACY

We developed a vertebra specific 3D printed drill guide based on MRI for placement of pedicle screws. Our results show that the conventional pedicle screw placement using these SpineGuide achieved an average deviation from the preplanned entry point of 2.29 mm and a mean angle deviation of 7.09˚, which is more than expected and unacceptable for clinical application. Thereby, only 11 of the 19 pedicle screws were fully inside the pedicle, although following Neo's classification 84.2% can be marked as safe. The results show a high variance in deviation of entry point and deviation of the angle. When comparing the left and right screw per SpineGuide there is a high variance and in most cases a nonsystematic deviation in entry point and angle per screw. Indicating that the SpineGuides are not tilted over one or more axis, but also deformed due to the flexibility of the material. Altogether the results show that the current SpineGuide is not accurate enough to safely insert pedicle screws in vertebrae.

Other studies showed a high accuracy in placement of pedicle screws using patient-specific drill guides. Most of the studies report an accuracy of over 90% Grade 0 and almost all of them 100% safe placements (Grade 0 + Grade 1) following Neo's classification by assessing the pedicle screw positions in CT, table 1. Thereby, Kong et al. and Lamartina et al. and Sugawara et al. report mean entry point deviation within 1 millimeter, which is much more accurate than the current SpineGuide [8–10]. Research by Takemoto et al. showed a high accuracy using titanium additive manufactured drill guides [18]. So, changes should be made in the manufacturing of the SpineGuide to improve its accuracy. For instance, a more rigid material for printing the drill guides, like titanium or stainless steel should be used, and the design by Swaan should be adopted for further development.

One of the potential advantages of the SpineGuide is that it is based on MRI. The use of MRI makes it possible to reduce radiation dose, which is of high importance in children and adolescents. In our study, we made use of the boneMRI protocol to visualize cortical bone. We segmented the vertebrae manually in these MRI slices, which is time-consuming (2.5 hours per vertebra). However, MRIguidance is currently working on an automatic segmentation algorithm to segment bony structures [26]. This would decrease the time needed to segment the vertebrae and will speed up to process of SpineGuide manufacturing.

Our study has several limitations in the design and use of the SpineGuide. First of all, in this study, we used a new design of the SpineGuide. We changed the SpineGuide design from a three point support guide to a five point support guide. We expected that a five point support guide would have a more stable fit. In hindsight, a five point support block needs more cleaning, especially of the transverse process. Takemoto et al. mentioned that drill guides designs with a large contact area might be more arduous to fit the local anatomy [18]. Cleaning of the transverse process is much more difficult than the lamina, because of ligamentous attachments. This results in more soft tissue being left behind on the transverse process and an unstable fit. Thereby, we did not use electrocauterization in the cleaning process, which is expected to give a better, cleaner result. Takemoto et al. had similar findings showing that support blocks only on the lamina and superior to the extremity of the spinous process should give a stable fit. The last is another limitation in the design of our SpineGuide. We changed the spinous process support block towards the posterior extremity of the spinous process instead of superior in the new design of the SpineGuide. The posterior extremity of the spinous process is a fibrous-cartilage like structure, which is not well distinguished in boneMRI, resulting in a less matched support block with the real anatomy. Thereby, this new place gave rise to the ability to tilt some of the SpineGuides, especially in the T9 and L3 SpineGuide. The support block superior to the extremity of the spinous process gives more rotational stability in all planes. Another limitation is the 3D print material (PA2200) which was not as rigid as expected. Some parts of the SpineGuides were really thin and this resulted in minor flexibilities and, therefore, less accurate drilling process. Finally, the holes were drilled with a standard drilling machine, which was also used for the insertion of the pedicle screws. The latter may have led to a less accurate placement of the pedicle screw due to the fact that the insertion speed is different than in manual insertion. A higher insertion speed may cause fracture of the cortex and therefore breakout of the pedicle screw.

A disadvantage in our accuracy analysis was the presence of several registration uncertainties. First, we manually matched the CT with the screws on the preoperative boneMRI. The datasets have different voxel and pixel dimensions, which makes manual registration difficult. It is expected that half of a CT pixel of 0.8 mm is the registration uncertainty. Second, in SolidWorks the segmented pedicle screws were matched on the vertebra with the preplanned trajectories. However, an odd deviation occurred during file transfer from MeVisLab to SolidWorks. The deviation was nonsystematic for each vertebra. Eventually, the odd deviation was solved with a registration uncertainty of 0.1 mm. So, a total registration uncertainty in the analysis of 0.5 mm has to be taken into account.

4.3 AXIAL DEROTATION WITH EXTREME SCREW POSITIONING

This study is primarily performed to investigate the use of extreme pedicle screws to aid in vertebral derotation. Ultimately, we want to use these screws to improve vertebral derotation in scoliosis surgery. The study showed that positioning preplanned extreme pedicle screws using a drill guide is feasible, despite the fact that the SpineGuide is not that accurate. Unfortunately, the extreme pedicle screws broke out during in the rotation maneuver resulting in no rotation of the vertebrae. The L2 pedicle screw stayed in place during the rotation maneuver, but no rotation was measured. Thereby, deformation of the rod did occur. This may be due to the lumbar vertebrae facet joints are not being anatomically orientated for rotational movement in the axial plane, resulting in all the forces acting on the rod causing deformation.

A limitation of our method is the consideration of using short spine segments of three vertebrae. Our thought was that we could do more measurements in one specimen using these short segments, increasing sample size. However, in scoliosis surgery 10 or more vertebrae are instrumented which gives more rotational and translational freedom of the apical vertebra. Thereby, forces will be distributed over more screws and longer rods, which makes pull-out of the pedicle screws less likely. For future research the study should be repeated with larger spine segments in multiple specimens, giving more translational en rotational movement and dividing the force over more instrumentation. Thereby, after we performed the first measurement on T3-T5, T7-T9, and T11-L1, we concluded that there was a high pull-out ratio and no visible rotation of the middle vertebra. Therefore, we choose the make an adjustment in our second measurement set, by removing the contralateral middle screw. We hypothesize that this screw fixed the middle vertebra, resulting in the pull-out of the extreme pedicle screw during rotation maneuver.

Another limitation of our study may be the method of fixation of the cephalad and caudal vertebra of each short spine segment. It was difficult to fix these vertebrae to a wooden beam using plastic bolts and nuts due to the small size of a vertebra and the shape of the spine. We managed to place a bolt through each vertebra, but it was hard to make direct contact between wooden beam and vertebrae to prevent any movement of the vertebra. We filled the gaps with wooden pieces and cork, but this was not as rigid as planned. Thereby, according the CT scans, some pieces of cork and wood touched some of the middle vertebrae, which may result in unwanted fixation of the middle vertebra. It is expected that a fixation method using 3D printed templates matching the anterior anatomy of the vertebral body can achieve better fixation. These templates can be attached to a wooden beam, without using wooden pieces and cork, keeping the middle vertebra free to move.

Measurements of the forces acting on the rod and extreme screw position was done with two methods. The measurement using the torque wrench had several uncertainties. The friction during the measurements varied and was greatly increased when the rod touched the screw head or the cricket itself. Thereby, several times the cricket disconnected from the screw head during measurement. Secondly, to obtain consistent results the torque wrench has to be turned with a constant angular speed, which is difficult by hand. The measurements by the FEM analysis had several limitations as well. The deformation of the rods was small (<1 mm) and measured in a 0.8 mm resolution of the CT. Thereby, several assumptions had to be made on the plastic-elastic characteristics of the CoCr rod, which make the FEM analysis less accurate; 20% deviation of material characteristics is possible. We compared the forces measured by the torque wrench with the FEM rod deformation analysis by Kuiper, Appendix 7.5 [47]. There were large differences in the two force measurements methods of 44%. The torque wrench partly overestimates the forces acting on the rods compared with the FEM in three cases (T3-T5, T7-T9, T9-T11). In two cases (T5-T7 and L1-L3) the forces are underestimated. Both measurement methods have a high uncertainty, so we were not able to approach reality. Again, longer spine segments may be a solution, because less force is needed to bend the rod and, therefore, less pull-out is expected. Thereby, longer rods bent more easily, so deformity of the rod should be measured more easily in CT.

An important limitation is the bone quality of the specimen used. We did not make a bone density scan beforehand, but chose a specimen with the least abnormalities on CT. The bone quality of a cadaver (57) is not comparable with an adolescent. Bone loss is accelerated after menopause in females, but this should not be a major issue in a 57-year female cadaver. The result may be that the bone could not withstand the forces acting on it during instrumentation and the rotation maneuver. This may happen partly by the bone quality itself, but is also influenced by the diameter of the screws used and the direction in which forces act on the screws. In our study we used 5.5 mm (T3-T6) and 6.5 mm (T7-L3) pedicle screws, which were in some cases not optimal for the pedicle they were inserted in. This may have led to a decreased fixation in the pedicles and vertebrae and, therefore, a decreased pull-out strength. Besides, in scoliosis surgery normally the force on the pedicle screw is directed axially, thereby making the best use of the screw thread and the ability to undergo high forces. Bianco and Aubin showed that nonaxial loading of pedicle screws leads to screw plowing and loosening of the pedicle screw, sometimes resulting in pullout or fractures [48]. In our case the force direction on the extreme pedicle screws is partly medially directed, which creates a high force on the medial bone-screw contact area, resulting in damage of the lamina. Thereby, the tip of the screw is expected to plow through the vertebral body. The room created by the wiggling of the extreme pedicle screw resulted in pull-out in four of five correctly placed extreme pedicle screws.

4.4 CONCLUSION

We performed a feasibility study on cadavers using extreme positioned pedicle screws to aid in vertebral rotation. The extreme pedicle screws were realized using preplanning of trajectories and patient-specific SpineGuides for drilling. The accuracy of the current SpineGuide is however unacceptable for clinical application. The influence of extreme pedicle screws on the axial vertebral rotation over short spine segments of three vertebrae could not be accomplished in our study. This may be a result of preliminary pullout of the extreme screws. Adjustment in the methods of the experiment should be made. The force was measured using a torque wrench and calculated using a FEM simulation. This approach showed a high variety in each segment and there is a variation between the force measurements by torque wrench and force FEM calculation.

4.5 FUTURE WORK

For future work we recommend the following points:

- Regarding the current SpineGuide:
    - Use a more rigid material or construction;
    - Use less contact areas and back to the tripod (three support blocks) design;
    - Use a support block on the superior surface of the spinous process;
    - Use a more automatically design and manufacturing process.
- Regarding the extreme pedicle screws to aid in vertebral derotation:
    - Use longer spine segments with more 'free' vertebrae;
    - Use more advanced measurement tools;
    - Use a better fixation technique for the vertebrae fixation;
    - Use a high bone density cadaver.

The design of the current SpineGuide should be adjusted to a more rigid structure. This could be done using rigid materials like titanium or stainless steel (which can be 3D printed as well) and by using thicker connections between the support blocks. Thereby, the 5 support block design should be adjusted back to the tripod (three support blocks) design, which has less contact areas limited to cortical bone surfaces. Additionally, the support block on the spinous process should be carefully chosen. It should be more superior to the extremity of the spinous process, but the cranial spinous process should not make contact with the support block. Finally, the current process of creating the volumes out of the boneMRI and manufacturing the SpineGuide is time consuming. Ideally, the MRI 3D volumes reconstructions of the vertebrae are created automatically. At this moment these automatic 3D reconstructions are not possible, but in the near future MRIguidance will make this available. Then, the process of planning the trajectories and creating the SpineGuide should be more user-friendly. These procedures are currently performed in open source software (MeVisLab and SolidWorks), but in the future this should be in a (self-made) software with user interface. In this user interface the surgeon should plan the trajectories in the 3D volumes (guided by the MRI images), chose the preferred diameter and length of the pedicle screw and the surgeon should point out the contact areas of the support blocks. The software should, preferably, create the SpineGuide automatically, where after it can be checked by a technician and the surgeon. If the software is fully working, validation of accuracy can be tested in cadavers and in a later stage clinically in patients.

The cadaver model with extreme pedicle screws to aid in vertebral derotation did no work as planned. We see several points which can be adjusted to make extreme pedicle screw placement a success. First, the longer spine segments with more 'free' vertebrae should be used, because it is expected that the forces are better distributed along the segments, preventing screw pullout. Thereby, the force measurements with the torque wrench and the force calculation with the FEM can be improved, for instance with more advanced measuring machines. Thereby, the material characteristics of CoCr should be more accurately determined, for example by using a three-point bending test in a calibrated force machine. Furthermore, it is expected that a fixation method using 3D printed templates matching the anterior anatomy of the vertebral body can achieve better fixation. These templates can be attached to a wooden beam, without using wooden pieces and cork, keeping the middle vertebra free to move. Finally, we did not measure the bone density of the 57-year female cadaver. In further studies it is recommended to measure the bone density in advance to the experiment to compare the results on the basis of the bone density of the cadaver. If the SpineGuide's accuracy is well assessed, further research can be performed with extreme pedicle screws in a cadaver model. For example by determining what the 'normal' rotation possibilities of vertebrae are in a human cadaver spine.

A final word regarding 3D printing in the medical world. 3D printing and planning are upcoming in medicine. We think that the technique of patient-specific 3D printing should be further developed in all hospitals and the UMC Utrecht should be a pioneer in this field. Especially the departments regarding the bony structures in the human body can gain a high advantage from 3D printing. For instance in the patient-specific treatment of fractures in which the 3D printing technique can be used to plan screw trajectories and reproduce them using drill templates, also casting could be replaced by 3D prints. Secondly, 3D printing could be helpful in the field of reconstruction surgery, for example, the planning of saw cuts and screw positions in mandibular reconstruction using the fibular bone. Thereby, 3D printing could also be used as patient-specific implants. More and more materials are suitable for sterile 3D printing, which could be implanted during surgery, for instance by spine stabilization surgery in kyphosis at risk.

5 ACKNOWLEDGEMENTS

Sebastiaan Wijdicks for thinking along and helping with the cadaver experiment

Simon Plomp for all the help at the anatomy department

Nils van Veen for all the help at the radiology department

Peter Seevinck and **Marijn van Stralen** for giving the opportunity to use boneMRI by MRIguidance

Rob Brink for thinking along in several steps of the analysis

Klaske Siegersma for revising my thesis

Jasper Drost for designing the SpineGuides and all the help with SolidWorks

Lisette van Steinvoren – Stamsnijder for all the guidance regarding the SpineGuide project

Ferdi van der Heijden for his presidency at my masters colloquium

The Orthopaedic Surgery department for the warm welcome and sociability during the thesis year

At last I want to thank **Moyo Kruyt**, **Edsko Hekman** and **Abel Swaan** for their intensive supervision and guidance during my whole thesis year and **Annelies Lovink** for guiding my personal development during two internship years.

6 REFERENCES

1. Smith PL, Donaldson S, Hedden D, et al. Parents' and patients' perceptions of postoperative appearance in adolescent idiopathic scoliosis. *Spine (Phila Pa 1976)*. 2006;31(20):2367-2374. doi:10.1097/01.brs.0000240204.98960.dd.

2. Qian B, Mao S, Zhu Z, et al. Antagonistic role of vertebral translation. *Spine (Phila Pa 1976)*. 2013;38(19):1201-1208. doi:10.1097/BRS.0b013e31829e0bf9.

3. Mao S, Qiu Y, Zhu Z, Zhu F, Liu Z, Wang B. Clinical evaluation of the anterior chest wall deformity in thoracic adolescent idiopathic scoliosis. *Spine (Phila Pa 1976)*. 2012;37(9):E540-E548. doi:10.1097/BRS.0b013e31823a05e6.

4. Hu Y, Yuan Z-S, Kepler CK, et al. Deviation Analysis of C1–C2 transarticular screw placement assisted by a novel rapid prototyping drill template. *J Spinal Disord Tech*. 2014;27(5):E181-E186. doi:10.1097/BSD.0000000000000087.

5. Hu Y, Yuan Z shan, Spiker WR, et al. A comparative study on the accuracy of pedicle screw placement assisted by personalized rapid prototyping template between pre- and post-operation in patients with relatively normal mid-upper thoracic spine. *Eur Spine J*. 2016;25(6):1706-1715. doi:10.1007/s00586-016-4540-2.

6. Jiang L, Dong L, Tan M, Yang F, Yi P, Tang X. Accuracy assessment of atlantoaxial pedicle screws assisted by a novel drill guide template. *Arch Orthop Trauma Surg*. 2016;136(11):1483-1490. doi:10.1007/s00402-016-2530-9.

7. Jiang L, Dong L, Tan M, et al. A Modified Personalized Image-Based Drill Guide Template for Atlantoaxial Pedicle Screw Placement: A Clinical Study. *Med Sci Monit*. 2017;23:1325-1333. doi:10.12659/msm.900066.

8. Kaneyama S, Sugawara T, Sumi M. Safe and accurate midcervical pedicle screw insertion procedure with the patient-specific screw guide template system. *Spine (Phila Pa 1976)*. 2015;40(6):E341-8. doi:10.1097/BRS.0000000000000772.

9. Kong X, Tang L, Ye Q, Huang W, Li J. Are computer numerical control (CNC)-manufactured patient-specific metal templates available for posterior thoracic pedicle screw insertion? Feasibility and accuracy evaluation. *Eur Spine J*. 2017:7. doi:10.1007/s00586-017-5215-3.

10. Lamartina C, Cecchinato R, Fekete Z, Lipari A, Fiechter M, Berjano P. Pedicle screw placement accuracy in thoracic and lumbar spinal surgery with a patient-matched targeting guide: a cadaveric study. *Eur Spine J*. 2015;24(7):937-941. doi:10.1007/s00586-015-4261-y.

11. Liu K, Zhang Q, Li X, et al. Preliminary application of a multi-level 3D printing drill guide template for pedicle screw placement in severe and rigid scoliosis. *Eur Spine J*. 2017;26(6):1684-1689. doi:10.1007/s00586-016-4926-1.

12. Lu S, Xu Y, Zhang Y. Application of a novel patient - specific rapid prototyping template in orthopedics surgery. In: *Advanced Applications of Rapid Prototyping Technology in Modern Engineering*. ; 2011:129-152. http://www.intechopen.com/books/advanced-applications-of-rapid-prototyping-technology-in-modernengineering/%5Cnapplication-of-a-novel-patient-specific-rapid-prototyping-template-in-orthopedics-surgery.

13. Lu S, Zhang YZ, Wang Z, et al. Accuracy and efficacy of thoracic pedicle screws in scoliosis with patient-specific drill template. *Med Biol Eng Comput*. 2012;50(7):751-758. doi:10.1007/s11517-012-0900-1.

14. Merc M, Drstvensek I, Vogrin M, Brajlih T, Recnik G. A multi-level rapid prototyping drill guide template reduces the perforation risk of pedicle screw placement in the lumbar and sacral spine. *Arch Orthop Trauma Surg*. 2013;133(7):893-899. doi:10.1007/s00402-013-1755-0.

15. Ma T, Xu YQ, Cheng Y Bin, et al. A novel computer-assisted drill guide template for thoracic pedicle screw placement: A cadaveric study. *Arch Orthop Trauma Surg*. 2012;132(1):65-72. doi:10.1007/s00402-011-1383-5.

16. Ryken TC, Owen BD, Christensen GE, Reinhardt JM. Image-based drill templates for cervical pedicle screw placement. *J Neurosurg Spine*. 2009;10(1):21-26. doi:10.3171/2008.9.SPI08229.

17. Sugawara T, Higashiyama N, Kaneyama S, et al. Multistep pedicle screw insertion procedure with patient-specific lamina fit-and-lock templates for the thoracic spine. *J Neurosurg Spine*. 2013;19(2):185-190. doi:10.3171/2013.4.SPINE121059.

18. Takemoto M, Fujibayashi S, Ota E, et al. Additive-manufactured patient-specific titanium templates for thoracic pedicle screw placement: novel design with reduced contact area. *Eur Spine J*. 2016;25(6):1698-1705. doi:10.1007/s00586-015-3908-z.

19. Yu Z, Zhang G, Chen X, et al. Application of a novel 3D drill template for cervical pedicle screw tunnel design: a cadaveric study. *Eur Spine J*. 2017. doi:10.1007/s00586-017-5118-3.

20. Chen HL, Wu DY, Yang HL, Guo KJ. Clinical use of 3D printing guide plate in posterior lumbar pedicle screw fixation. *Med Sci Monit*. 2015;21:3948-3954. doi:10.12659/MSM.895597.

21. Chen H, Guo K, Yang H, Wu D, Yuan F. Thoracic pedicle screw placement guide plate produced by three-dimensional (3-D) laser printing. *Med Sci Monit*. 2016;22:1682-1686. doi:10.12659/MSM.896148.

22. Farshad M, Betz M, Farshad-Amacker NA, Moser M. Accuracy of patient-specific template-guided vs. free-hand fluoroscopically controlled pedicle screw placement in the thoracic and lumbar spine: a randomized cadaveric study. *Eur Spine J*. 2017;26(3):738-749. doi:10.1007/s00586-016-4728-5.

23. Putzier M, Strube P, Cecchinato R, Lamartina C, Hoff E. A new navigational tool for pedicle screw placement in patients with severe scoliosis: a pilot study to prove feasibility, accuracy, and identify operative challenges. *J Spinal Disord Tech*. 2014;30(4):430-439. doi:10.1097/BSD.0000000000000220.

24. Smith & Nephew. VISIONAIRE Technology Cutting Guides for Knee Replacement. 2017. http://www.smith-nephew.com/professional/products/all-products/visionaire-technology/visionaire/. Accessed August 21, 2017.

25. Swaan A. Development of a MRI-based personalized drill guide for pedicle screws in scoliotic thoracic vertebrae. 2012.

26. Seevinck P, Stralen M van, Raatgever R. MRIguidance. mriguidance.com. Accessed August 21, 2017.

27. Geldof F. Comparing vertebral segmentation accuracy of new MRI sequences with CT to find the imaging technique resulting in the best 3D segmentation for the SpineGuide. 2017.

28. Holland Innovative. Holland Innovative - Integrated Product Development. https://www.holland-innovative.nl/. Accessed August 21, 2017.

29. Drost J. SpineGuide. 2017.

30. Konieczny MR, Senyurt H, Krauspe R. Epidemiology of adolescent idiopathic scoliosis. *J Child*

Orthop. 2013;7(1):3-9. doi:10.1007/s11832-012-0457-4.

31. Wang W, Baran GR, Betz RR, Samdani AF, Pahys JM, Cahill PJ. The use of finite element models to assist understanding and treatment for scoliosis: A review paper. *Spine Deform*. 2014;2(1):10-27. doi:10.1016/j.jspd.2013.09.007.

32. Cheng JC, Castelein RM, Chu WC, et al. Adolescent idiopathic scoliosis. *Nat Rev Dis Prim*. 2015;1(October 2016):15030. doi:10.1038/nrdp.2015.30.

33. Davies G, Reid L. Effect of scoliosis on growth of alveoli and pulmonary arteries and on right ventricle. *Arch Dis Child*. 1971;46:623-632. doi:10.1136/adc.46.249.623.

34. Tsiligiannis T, Grivas T. Pulmonary function in children with idiopathic scoliosis. *Scoliosis*. 2012;7(1):7. doi:10.1186/1748-7161-7-7.

35. Liljenqvist UR, Allkemper T, Hackenberg L, Link TM, Steinbeck J, Halm HFH. Analysis of vertebral morphology in idiopathic scoliosis with use of magnetic resonance imaging and multiplanar reconstruction. *J Bone Joint Surg Am*. 2002;84-A(3):359-368. http://eutils.ncbi.nlm.nih.gov/entrez/eutils/elink.fcgi?dbfrom=pubmed%7B&%7Did=11886904%7B&%7Dretmode=ref%7B&%7Dcmd=prlinks.

36. Chang MS, Lenke LG. Vertebral derotation in adolescent idiopathic scoliosis. *Oper Tech Orthop*. 2009;19(1):19-23. doi:10.1053/j.oto.2009.04.001.

37. Pratt RK, Webb JK, Burwell RG, Cole AA. Changes in surface and radiographic deformity after Universal Spine System for right thoracic adolescent idiopathic scoliosis: is rib-hump reassertion a mechanical problem of the thoracic cage rather than an effect of relative anterior spinal overgrowth. *Spine (Phila Pa 1976)*. 2001;26(16):1778-1787.

38. Lee SM, Suk SI, Chung ER. Direct vertebral rotation: a new technique of three-dimensional deformity correction with segmental pedicle screw fixation in adolescent idiopathic scoliosis. *Spine (Phila Pa 1976)*. 2004;29(3):343-349. doi:10.1097/01.BRS.0000109991.88149.19.

39. Fu G, Kawakami N, Goto M, Tsuji T, Ohara T, Imagama S. Comparison of vertebral rotation corrected by different techniques and anchors in surgical treatment of adolescent thoracic idiopathic scoliosis. *J Spinal Disord Tech*. 2009;22(3):182-189. doi:10.1097/BSD.0b013e318177028b.

40. Asghar J, Samdani AF, Pahys JM, et al. Computed tomography evaluation of rotation correction in adolescent idiopathic scoliosis: a comparison of an all pedicle screw construct versus a hook-rod system. *Spine (Phila Pa 1976)*. 2009;34(8):804-807. doi:10.1097/BRS.0b013e3181996c1b.

41. Hwang SW, Samdani AF, Cahill PJ. The impact of segmental and en bloc derotation maneuvers on scoliosis correction and rib prominence in adolescent idiopathic scoliosis. *J Neurosurg Spine*. 2012;16(4):345-350. doi:10.3171/2011.11.SPINE11277.

42. Rushton PRP, Grevitt MP. Do vertebral derotation techniques offer better outcomes compared to traditional methods in the surgical treatment of adolescent idiopathic scoliosis? *Eur Spine J*. 2014;23(6):1166-1176. doi:10.1007/s00586-014-3242-x.

43. Gregersen GG, Lucas DB. An in vivo study of the axial rotation of the human thoracolumbar spine. *J Bone Jt Surg*. 1967;49.

44. Haher TR, O'Brien M, Felmly WT, et al. Instantaneous axis of rotation as a function of the three columns of the spine. *Spine (Phila Pa 1976)*. 1992;17(6 Suppl):S149-54. doi:10.1097/00007632-199206001-00015.

45. White III AA, Panjabi MM. The clinical biomechanics of scoliosis. *Clin Orthop Relat Res*. 1976.

46. Badve SA, Ordway NR, Albanese SA, Lavelle WF. Toward a better understanding of direct vertebral rotation for AIS surgery: Development of a multisegmental biomechanical model and factors affecting correction. *Spine J*. 2015;15(5):1034-1040. doi:10.1016/j.spinee.2014.12.002.

47. Kuiper R. Chapter 3 Spinal Rod Instrumentation. 2017.

48. Bianco R-J, Aubin C-E, Mac-Thiong J-M, Wagnac E, Arnoux P-J. Pedicle screw fixation under nonaxial loads. *Spine (Phila Pa 1976)*. 2016;41(3):E124-E130. doi:10.1097/BRS.0000000000001200.

49. MeVis Medical Solutions AG, MEVIS F. MeVisLab - development environment for medical image processing and visualization. www.mevislab.de.

50. Dassault Systèmes SolidWorks Corporation. Solidworks. http://www.solidworks.com.

51. Oceanz. Oceanz - your 3D printing professional. www.oceanz.eu.

52. K2M Inc. K2M - complex spine innovations. www.k2m.com.

53. Neo M, Sakamoto T, Fujibayashi S, Nakamura T. The clinical risk of vertebral artery injury from cervical pedicle screws inserted in degenerative vertebrae. *Spine (Phila Pa 1976)*. 2005;30:2800-2805.

54. Microsoft. Microsoft Excel 2013. www.microsoft.com.

55. The Mathworks Inc. MATLAB 2015 - MathWorks. *www.mathworks.com/products/matlab*. 2016. doi:2016-11-26.

56. Medacta International SA, Castel San Pietro C. MySpine. 2017.

7 APPENDIX

7.1 APPENDIX 1 – SEGMENTATION VERTEBRAE MEVISLAB

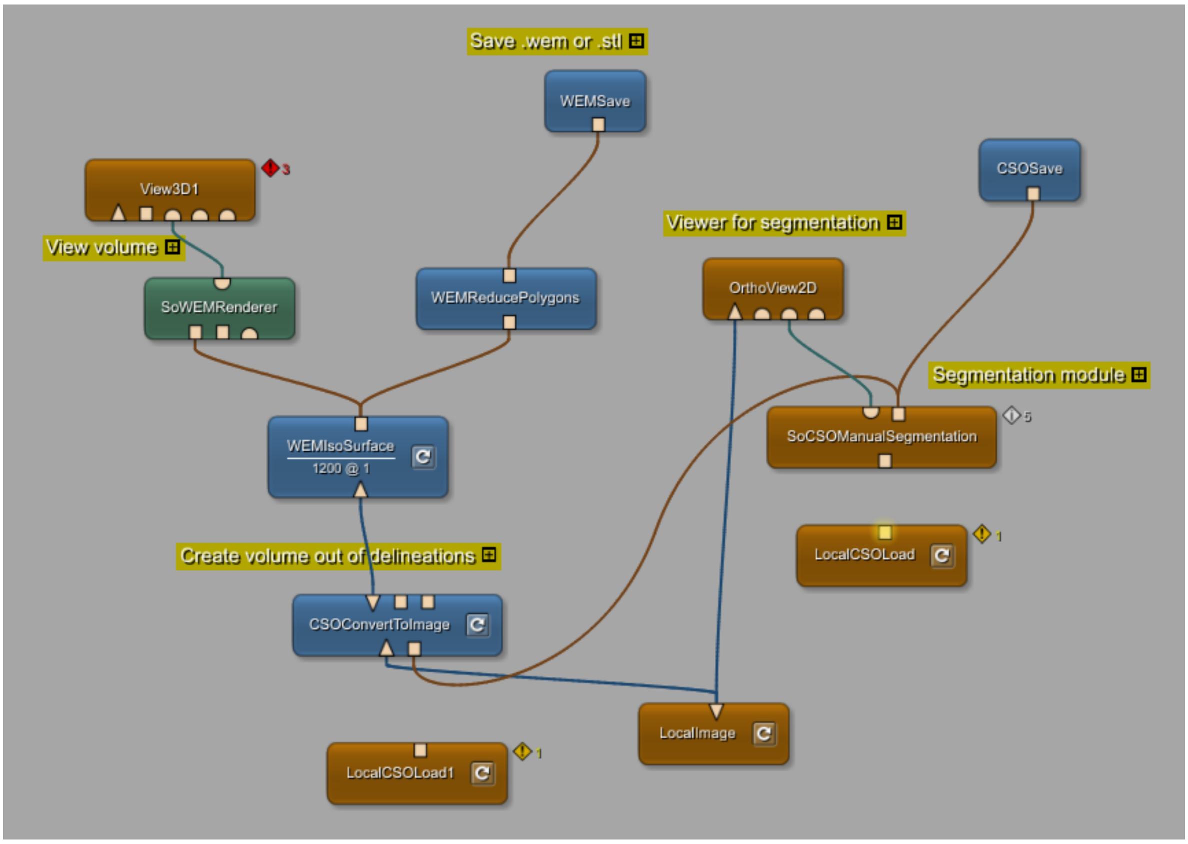

The network used in MeVisLab for segmentation of the vertebrae in boneMRI is shown above. A dataset can be loaded using the 'LocalImage' module. Labels, description and groups can be created in the 'SoCSOManualSegmentation' module. A spline interpolation line is used for the manual segmentations. The delineations of the vertebrae is done in the 'OrthoView2D' module. The vertebrae is delineated in the axial plane for each slice. The delineations are automatically stored in the 'SoCSOManualSegmentation' module when the delineation loop is closed. The delineation can be saved with the 'CSOSave' module when ready. A volume can be created on the left side of the network. The delineations are loaded into the 'CSOConvertToImage' to make the delineations solid. Then, the 'WEMIsoSurface' module is used to create polygons in the surface, which automatically smoothens the volume. The volume with polygons can be reduced to speed up post-processing steps, but this could make the surface of the volume less accurate. The 'WEMSave' module is used to save the volumes in .wem- or .stl-files.

Sidenote: An assumption made was that the cortical bone on boneMRI was imaged as a no-signal area (black), because there is a low amount of free water in cortical bone, and these areas were included in the segmentations.

7.2 APPENDIX 2 – TRAJECTORY PLANNING SOLIDWORKS

A tutorial video is available for trajectory planning in SolidWorks. In the video the following steps are performed after loading the .stl-file of a vertebra:

1. Define a plane through the pedicle
2. Draw a line in the plane through the pedicle
3. Define a second plane orthogonal on the end of the line
4. Create a circle in the second plane with the diameter of the screw
5. The circle can be used to cut out a cylinder all along the line.
6. Step 1 to 5 can be repeated for the other pedicle.

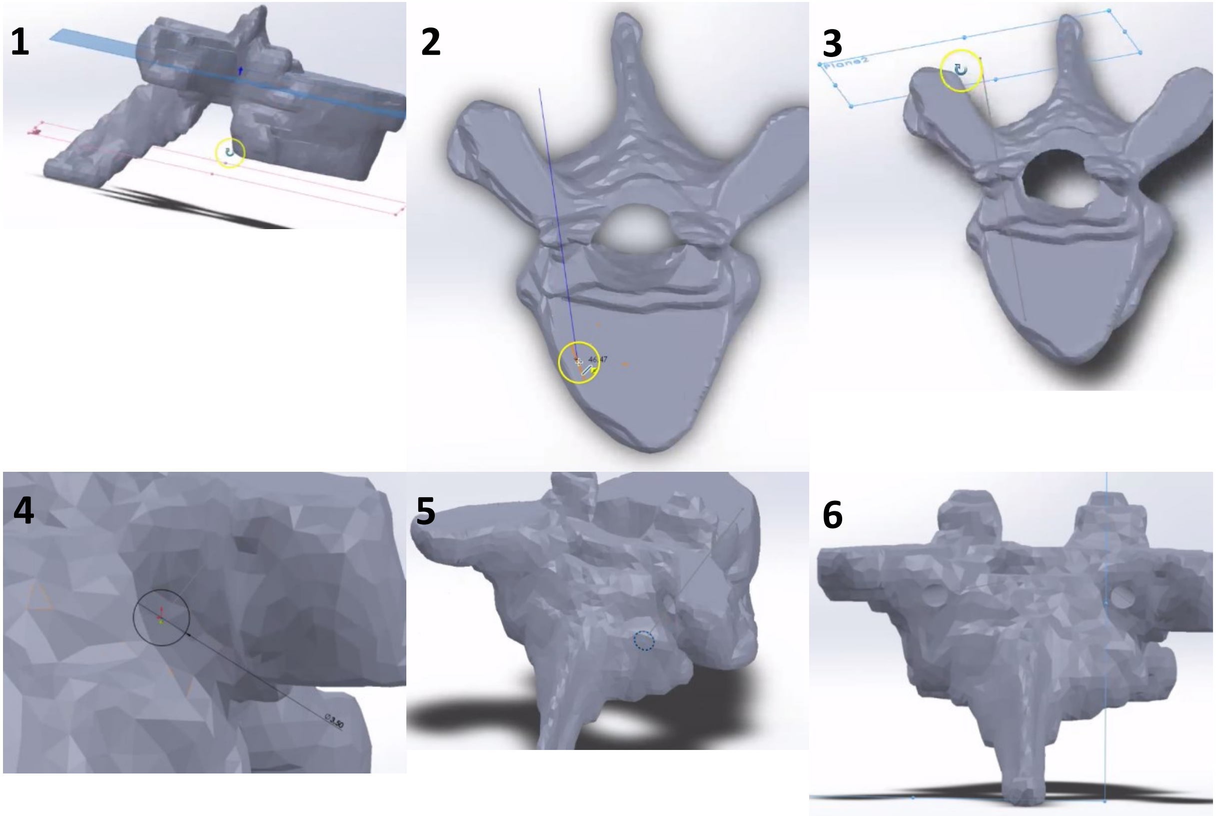

Afterwards, the pedicle screw trajectories are verified by an experienced orthopaedic surgeon. Conventional trajectories are based on literature about screw placement.

7.3 Appendix 3 – SpineGuide design SolidWorks

A tutorial video is available for design of the SpineGuide in SolidWorks. In the video the following steps are performed after the trajectory planning is executed:

1. Create a rectangle in the plane orthogonal on the trajectory
2. Use the 'extrude' function to expand the rectangle to the surface of the vertebra
3. A support block is created
4. Repeat step 1 to 3 for the second support block
5. Create a plane through the spinous process in the sagittal plane
6. Use the 'loft' function to create a bridge from the first support block towards the plane in the spinous process and then towards the second support block
7. A SpineGuide with three support blocks designed by Swaan is now created.

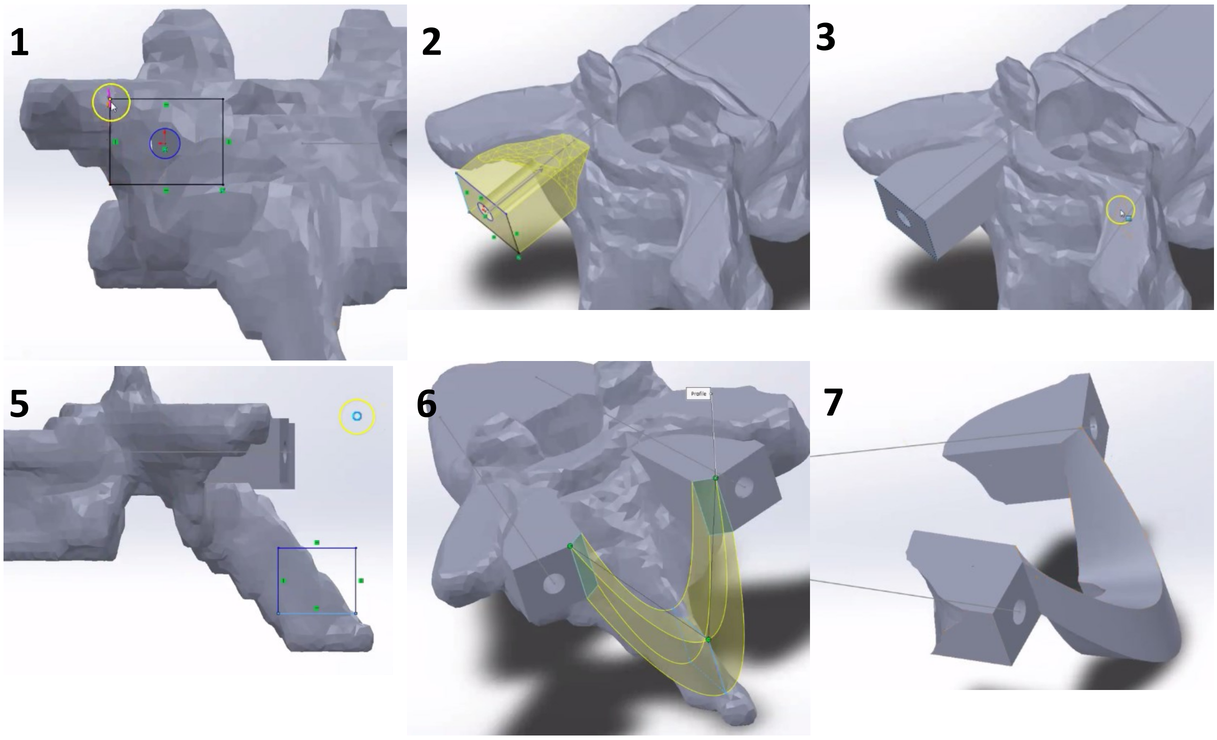

7.4 APPENDIX 4 – CALIBRATION CRICKET

To use the torque wrench in the experiment to measure force, a calibration had to be performed. We created a weigh scale unit and attached this unit to the cricket. The unit did only had contact with the cricket and with nothing else. Then, we putt weights on the weigh scale unit and measures the torque needed to lift this amount of weight plus the weight of the weigh scale unit. We repeated these step for multiple different weights and measures multiple times. We used lubricate oil to lessen the friction coefficient.

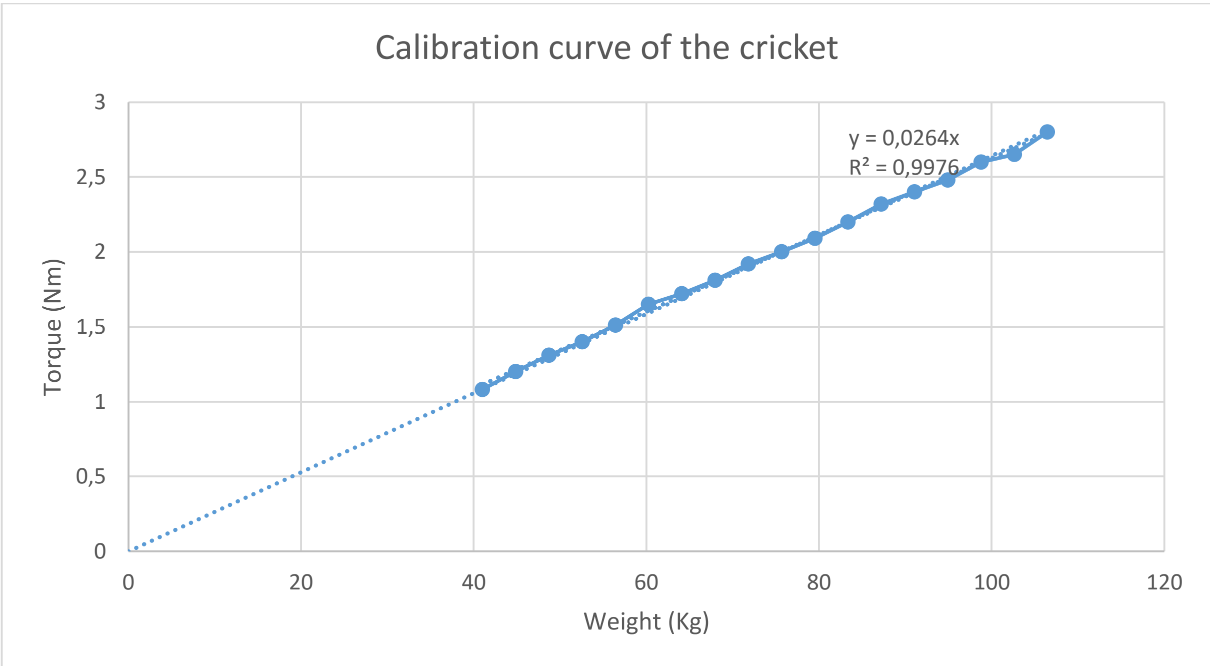

The following step was to determine the translation from torque to force and the influence of the friction coefficient. Therefore, we measured the pith of the cricket and the diameter of the cricket screw thread. We used the following formula to determine the expected relation from torque to force:

$$Force_{axial} = \frac{Torque}{Arm} \times \frac{Circumference}{Pitch}$$

a. Force (N) = weight (Kg) on weigh scale unit times earths standard gravity (9.81)
b. Torque = the expected torque calculated using the formula (without any friction coefficients)
c. Arm = the radius of the bolt in the cricket (0.0031 m)
d. Circumference = circumference of the bolt in the cricket (2π x radius bolt = 0.019 m)
e. Pitch = axial displacement of the bolt after one 360 degree turn (0.002536 m)

For every weight we used, we calculated the expected torque needed to lift this weight. Second, we compared this expected torque with the torque we measured using the weigh scale unit. Hereby, we determined that ±89% of the torque is used to conquer the friction coefficient, but still the friction coefficient varied between repeated measurements..

7.5 Appendix 5 – FEM simulation by Kuiper

Partly copied 'Chapter 3' from master thesis Kuiper.

7.5.1 Research Objective

Aim Estimate and evaluate the forces experienced by implant rods during operative scoliosis correction, to validate and improve an existing finite element method model of the scoliotic spine.

Motivation FEM models of the spine have the potential to improve the design and effectiveness of treatment. However, these models must be validated before accurate predictions of treatment outcome can be made. By measuring the deformation of implanted rods with a known stiffness, the stiffness of the spine can be deduced. This can be compared to the stiffness predicted by the FEM model.

Sub-Aim 1: Force measurements

Aim Estimate the forces acting on rod instrumentation implanted into cadaveric spinal segments through a FEM model.

Motivation The reaction forces in the implant rods can be derived from their deformation in situ by use of a FEM model. These reaction forces combined with the deformation of the spine can be used as a measure of stiffness of the spinal segment.

Assessment CT-scans are made of rod instrumentation before and after implantation in cadaveric spinal segments. The deformation of the rods is modelled using FEM. The reaction forces are taken from the model.

7.5.2 Finite Element Method

FEM models are made in Abaqus. The spine model is based on the model originally developed by Gerdine Meijer.

Model 1: A FEM model is constructed of the rods, with material properties as described in Appendix B. The geometry of the rods is based on the scans from CT 1. The deformation of the 6 in situ rods as observed in CT 2 and CT 3 are simulated by applying a displacement to the point of attachment of the distal screw. The forces acting on the screws are then derived from the reaction forces in the model.

Thereafter, the displacement constraints are removed. The contributions of plastic and elastic deformation are then established.

7.6 APPENDIX 6 – SPINEGUIDE ACCURACY ANALYSIS

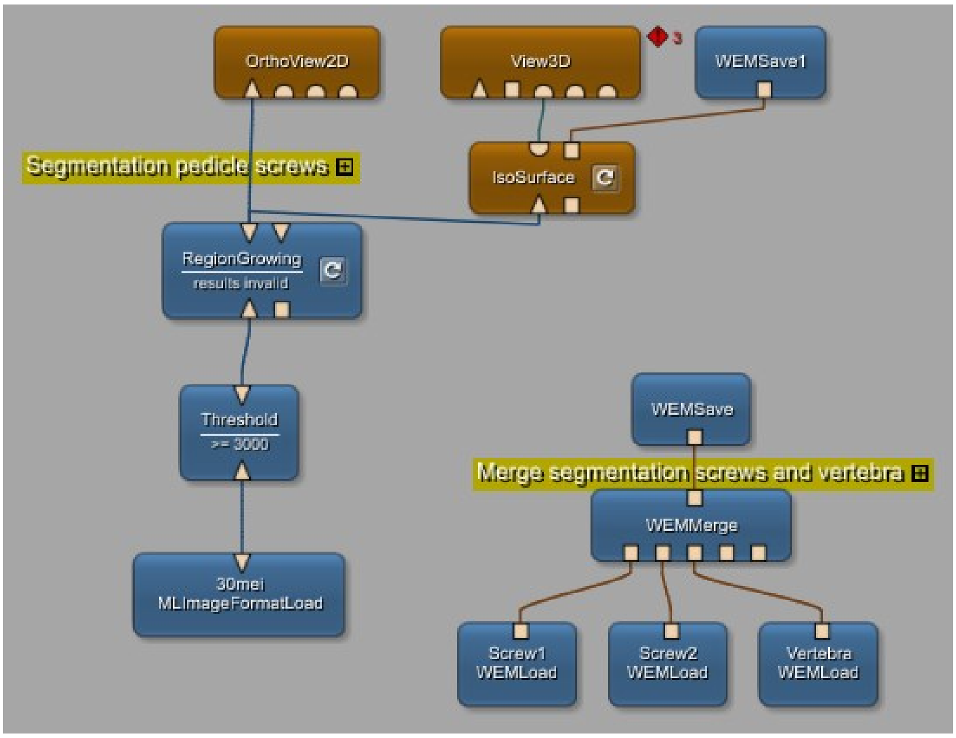

The SpineGuide analysis is performed in MeVisLab and SolidWorks. First, the CT of time point 1 is loaded and manually registered on the preoperative boneMRI by aligning the vertebra. The world coordinates of the CT are now transformed to the world coordinates of the preoperative boneMRI. The 'registered' CT is saved as 'MLImageFormat'. A separate registration is done for each vertebra.

The 'MLImageFormat' is loaded in the network shown above. First, a threshold is executed so only pixels of 3000 Hounsfield Units or higher are left. Then, a coordinate of a pixel inside the first screw is selected. This pixel is used to start a region growing segmentation via the 'RegionGrowing' module. A volume is created of the pedicle screw and the volume is saved as a .wem-file. These steps are repeated for both pedicle screws. At last, the .wem-files of the two pedicle screws and the segmentation of the vertebra in the preoperative boneMRI are combined and saved as a .stl-file (see sidenote).

The following steps are executed in SolidWorks. The .stl-file with the segmentation of the boneMRI vertebra with the trajectory planning is loaded. Then, the .stl-file with the segmented pedicle screws is added. Both .stl-files have the volume of the same vertebra, so matching of these vertebra could be done. The pedicle screw positions can now be compared with the preoperative planned trajectories.

The comparison is done in SolidWorks as well. A plane is created exactly through the center of the pedicle screw over its length. Then, a line is drawn in this plane which runs through die axial center of the pedicle screw. This is done for both pedicle screws. Second, the angle between the line through the screw and the preoperative trajectory is calculated, which is the angle deviation. Furthermore, the deviation of entry point is measured by taking the distance between the line through the pedicle screw and the preoperative trajectory. The shortest distance at the height of the lamina is taken, which is the entry point deviation.

Sidenote: Normally, when the screws are segmented in MeVisLab, they could be transferred to SolidWorks without merging the segmentation of the vertebra to the segmentation of the pedicle screws in MeVisLab. However, in our case this transfer gave us an odd and non-systemic 'extra' deviation in SolidWorks. The solution was to merge the preoperative vertebra segmentation with the segmentation of the pedicle screws in MeVisLab. The volume of the vertebra can be used for aligning the pedicle screws in the preoperative planning.

7.7 Appendix 7 – Torque measurements

Table 4 – Torque per quarter turn measured with a torque wrench. In brackets the force translated using the cricket calibration curve.

Short Spine Segment	Turn 1 Nm (N)	Turn 2 Nm (N)	Turn 3 Nm (N)	Turn 4 Nm (N)	Turn 5 Nm (N)	Turn 6 Nm (N)	Turn 7 Nm (N)	Turn 8 Nm (N)	Turn 9 Nm (N)	Turn 10 Nm (N)	Turn 11 Nm (N)
T3-T5	0.76 (282)	1.03 (383)	1.34 (498)	1.69 (628)	1.95 (725)	2.17 (806)	2.38 (884)	2.71 (1007)			
T5-T7	0.56 (208)	0.60 (223)	0.73 (271)	0.86 (320)	0.99 (368)	1.06 (394)	1.11 (412)	1.49[a] (554)	1.60 (595)	2.51 (933)	2.61 (970)
T7-T9	0.52 (193)	0.59 (219)	0.74 (275)	1.04 (386)	1.20 (446)	1.48[b] (550)	1.84 (684)				
T9-T11	0.62 (230)	0.72 (268)	0.94 (349)	1.12 (416)	1.18 (438)	1.23[c] (475)					
L1-L3	0.86 (320)	1.18 (438)	1.42 (528)	1.55 (576)	3.83[d] (1423)						

Note: a Pullout screw noticed |b Pullout screw noticed |c Cricket disconnected |d Rod touched screw head